POLITECNICO DI TORINO

CORSO DI LAUREA MAGISTRALE IN INGEGNERIA ENERGETICA E NUCLEARE

TESI DI LAUREA MAGISTRALE

Centralized and distributed generation in a district heating system: application of a thermal and fluid-dynamic model for integrated energy network analysis

Relatore
Prof. Pierluigi Leone

Corelatori
Dott. Marco Cavana
Dott. Enrico Vaccariello

Candidato
Andrea Cascavilla

A.A. 2019/2020

Ad Alessia
Alla mia famiglia

Abstract

The aim of this work is to implement and apply a model to evaluate the thermo-fluid dynamic behaviour of district heating networks, with the help of graph theory and SIMPLE algorithm.

The purpose of this implementation is to study the feasibility of the substitution of natural gas users with district heating users, in order to study the possibility of an integrate energy network analysis.

The first part of the work is dedicated to the numerical implementation, with the help of software Matlab, of the physical problem. A generic network is analyzed, with consequent results and validation of the model.

Once the model is validated, it has been applied to a real configuration: a case study of a gas network in an urban area. A substitution of natural gas load for heating with district heating is supposed. The installation of the network is studied in two different configurations: centralized heat generation and distributed heat generation.

In the first case a cogeneration plant of 90 MWe is chosen, where the heat generated is provided to the district heating network and the electricity generated is sent to the grid.

In the second case the power of the cogeneration plant is halved, the supply temperature of the grid is decreased and 21 thermal boosters are applied in strategic nodes. These thermal boosters are linked to the gas network and electricity grid, and here space for an integrate energy network analysis is left.

The study ends with the analysis of Carbon Dioxide emissions, primary energy saving and economic analysis of the two different installation configurations.

Contents

List of Figures

List of Tables

1 Introduction

District heating systems can be defined as the distribution of thermal energy from a central source to residential or industrial activities.
In the last 50 years this technology spread all over the world, specially in USA, Europe, Japan, China and Korea. Only in Europe it reaches more than 60 million people.
Various sources of heat supply these kind of systems: cogeneration, industrial waste heat, incinerators, solar energy, biomass. Thanks to these sources district heating is more environmentally-friendly than boilers in single houses: every year more than 5000 district heating systems in Europe, covering more than 10% of total European heat demand [2], contributes to avoid 3-4% of CO_2 emissions [1].

This situation makes district heating of topical interest, in the field of energetic transition and environmental issue. For this reason research in this area is going toward an integration with green energy, that brings in the study not only district heating network, but also electricity grid and gas network. A lot of publications address the problem of synergy for all the energetic networks. In this regard the 4^{th} generation district heating is a central point [3]: the district heating is integrated with smart technologies, smart metering, storage and renewables, in order to obtain a more green and efficient system.

In the area of smart energy, analyses on the *prosumers* in district heating have been conducted [4], studying the impact of including someone who both consumes and produces heat in a local network. Nevertheless, for the objective of this work, the most interesting studies are those ones involving other networks. The integration in smart energy systems, in fact, allows solutions of low-cost storage and consequently a participation in balancing fluctuating renewable energy sources [5], like the solution proposed by Rehman et al. [6], in which a photovoltaic distributed and three solar thermal district heating systems are compared, showing that the first overcomes all the others in terms of economic and environmental aspects.

A solution of great interest is the combination of combined heat and power (CHP) plants together with large scale heat pumps in district heating systems to balance intermittent renewable power production [7]. It is possible to use power production and consumption to balance both surplus and deficit in the electric power market. This is the case of integration of the three energetic networks, whose behaviour can be analyzed by computational studies.
Remaining in the field of green and circular economy, a form of integration is also using biogas from wastewater treatment plant as a source of heat for the network [8].

Concerning numerical design of district heating network several studies have been conducted. In this work the method proposed by Sciacovelli, Verda and Borchiellini [9] has been taken as reference. This method allowed to implement numerical codes in Matlab for the calculation, in steady and unsteady state, of temperature, mass flow rate and pressure of the district heating network taken into account.

2 Numerical model of district heating networks

2.1 Physical problem

The analysis of a district heating network involves the prediction of mass flow rate, temperature and pressure, evaluated in some specific points, according to what is needed. The purpose of this study is the modeling of the behaviour of the district heating network in connection with electrical grid and gas network.
A physical and then numerical model is necessary to assess all the things above mentioned, because installing measuring equipment on the networks to measure the quantities needed at various locations would be too expensive, intrusive and therefore complicated.

The model chosen is a *quasi-dynamic model* [10]: the thermal problem is simulated in unsteady state, while the fluid-dynamic formulation is considered stationary. This because the hydraulic perturbations are transferred in a time of few seconds, which is even smaller than the time step adopted. On the contrary, thermal perturbations travel at the fluid velocity, so the effect are slower and remarkable for this study. The approach used in this study follows the one proposed by Sciacovelli, Verda and R.Borchiellini [9].

The model is based on the conservation equations:

1. CONTINUITY EQUATION

   In differential form:

$$\frac{d\rho}{dt} + \rho \nabla \cdot \mathbf{u} = 0 \ , \tag{1}$$

   which in case of one-dimensional formulation becomes:

$$\frac{\partial \rho}{\partial t} + \frac{\partial(\rho v_1)}{\rho x_1} = 0 \ . \tag{2}$$

2. MOMENTUM EQUATION

In differential form the equation is

$$\rho \frac{Dv}{Dt} = -\nabla p - \nabla \cdot \tau + F \ , \tag{3}$$

that, written for one dimension along x_1 direction, becomes:

$$\rho \frac{\partial v_1}{\partial t} + \rho v_1 \frac{\partial v}{\partial x_1} = -\frac{\partial p}{\partial x_1} - F_{fr} + F_1 \ , \tag{4}$$

where F_{fr} identifies distributed pressure drop and $F_1 = \rho \cdot g_{x_1} - F_{local} + F_{pump}$ is the source term, including gravity, local pressure drop and pressure rise due to pumps.

3. ENERGY CONSERVATION EQUATION
   In differential form, with compressibility effect and viscous heating assumed negligible and with constant properties:

$$\frac{\partial(\rho c_p T)}{\partial t} + \nabla \cdot (\rho c_p \mathbf{u} T) = \nabla^2 k T + Q_s \ , \tag{5}$$

where the second term is the advective term, the third is the conductive term and the fourth is the volumetric heat source. Written for one dimension x_1:

$$\frac{\partial(\rho c_p T)}{\partial t} + \frac{\partial(\rho c_p u_1 T)}{\partial x_1} = k \frac{\partial^2 T}{\partial x_1^2} + Q_v - Q_l \ , \tag{6}$$

where Q_v identifies the heat generated inside the system, while Q_l the heat losses.

2.2 Numerical problem

In order to implement this model, the structure of a district heating network is described with the help of the **graph theory**. A *graph* is a set of objects connected through each others: the objects are called *nodes*, and each node can be connected to

other nodes through multiple links, called *branches*. For a district heating network, nodes correspond to junctions, and branches, elements that link to different nodes, correspond to pipes, ducts and similar components. The best way to describe the network topology of a flow network, i.e. the interconnections between nodes and branches, is the *incidence matrix* **A**, where the general element A_{ij} is equal to:

- 1, if the i-th node is the inlet node of j-th branch;
- -1, if the i-th node is the outlet node of j-th branch;
- 0, if there is no connection between node i and branch j.

It follows that matrix A has a number of rows equal to the number of nodes and number of columns equal to the number of branches.

2.2.1 Fluid dynamic problem

In order to calculate the mass flow rates in the network mass conservation equation is needed. If equation (1) is integrated over a control volume CV that includes one node and half of each branch connected to it, one can obtain:

$$\frac{dM}{dt} + \sum_{j=1}^{NB} \rho_j \cdot v_{1,j} \cdot S_j = 0 \ , \tag{7}$$

where M is the mass of fluid in the control volume, NB is the total number of branches, S_j is the j-th branch cross section.
In order to consider a possible injection or extraction of the fluid from a node, the term G_{ext} is added, which represent the mass flow rates exiting from the junctions (in this case it is a positive term) or entering (negative term). Considering also the definition of mass flow rate it is obtained: the following expression:

$$\frac{dM}{dt} + \sum_{j=1}^{NB} G_j + G_{ext} = 0 \ , \tag{8}$$

considering then steady-state condition for the fluid dynamic problem:

$$\sum_{j=1}^{NB} G_j + G_{ext} = 0 \ . \tag{9}$$

Applying the equation (9) to every element of the network, in matrix form:

$$\mathbf{A} \cdot \mathbf{G} + \mathbf{G}_{ext} = 0 \ , \tag{10}$$

where $\mathbf{G}$ is a column vector with dimension equal to the number of branches that identify the mass flow rate in every branch, and $\mathbf{G}_{ext}$ is a column vector whose i-th element correspond to the mass flow rate extracted (positive value) or injected (negative value) in node i; if no mass flow rate is exiting or entering the i-th node, i-th element is null. Its dimension is equal to the number of nodes.

In the case of **unsteady state** conditions it is necessary to discretize in time the time-dependent term. In order to do that Backward Euler method is chosen, implicit but unconditionally stable.
Thus the equation (8), with mass M expressed as $M = \rho V$, becomes:

$$\frac{d\rho}{dt} V_i + \sum_{j=1}^{NB} G_j + G_{ext} = 0 \ , \tag{11}$$

that, discretized with Backward Euler, is:

$$\frac{\rho^t - \rho^{t-\Delta t}}{\Delta t} V_i + \sum_{j=1}^{NB} G_j^t + G_{ext}^t = 0 \ , \tag{12}$$

and in matrix formulation:

$$\mathbf{A} \cdot \mathbf{G}^t + \mathbf{G}_{ext}^t + \mathbf{r}^t \ . \tag{13}$$

In this case density is considered constant in time, so this formulation is redundant and it results equal to the one expressed in equation (10).

The momentum equation is used to calculate pressure drop in the network. After the integration over a control volume that includes two nodes and branch that links them, the equation (4) becomes:

$$\rho\frac{\partial v_1}{\partial t}SL + \rho\frac{v_{1,out}^2 - v_{1,in}^2}{2}S = (p_{in} - p_{out})S - \rho g(z_{out} - z_{in})\cdot S - \Delta P_{fr}\cdot S \\ - \Delta P_{local}\cdot S + \Delta P_{pump}\cdot S \ , \tag{14}$$

where S is the cross section, L is the length of the branch.
By introducing the total pressure $P = p + \rho\frac{v^2}{2} + \rho g z$ and by eliminating the time dependent term (steady state) the equation (14) can be written as:

$$(P_{out} - P_{in}) = -\Delta P_{fr} - \Delta P_{local} + \Delta P_{pump} \ , \tag{15}$$

where distributed pressure drop can be expressed according to Darcy-Weisbach formula:

$$\Delta P_{fr} = \frac{1}{2}\lambda\frac{L}{d}\rho v_1^2 \ , \tag{16}$$

with λ Darcy friction factor, d hydraulic diameter of the pipe; concentrated pressure drop can be expressed as:

$$\Delta P_{local} = \frac{1}{2}\sum_k \zeta_k \rho v_1^2 \ , \tag{17}$$

where $\sum_h \zeta_k$ is the sum of all loss coefficient.
The Darcy friction factor is calculated as follows:

- Laminar flow: $\lambda = \dfrac{64}{Re_e}$
- Turbulent flow: in this case the friction factor λ is function of Reynolds number e relative roughness. The Colebrook-White formula has to be used, but it is an implicit function and so it has to be calculated iteratively imposing a proper tolerance.

$$\frac{1}{\sqrt{\lambda}} = -2\cdot log\left(\frac{2.51}{Re\cdot\sqrt{\lambda}} + \frac{\epsilon/d}{3.7}\right) \tag{18}$$

Substituting then equations (16) and (17) in (15) and applying at the control volume that includes a branch and the two nodes at the extremities it is obtained:

$$(P_{i-1} - P_i) = \frac{1}{2}\frac{G_j^2}{\rho S_j^2}(\lambda_j \frac{L_j}{d_j} + \sum_k \zeta_{k,j}) - \Delta P_{pump,j} \tag{19}$$

Applying equation (19) at every branch j of the network and defining hydraulic resistance as $R_j = \frac{1}{2}\frac{G_j}{\rho S_j^2}(\lambda_j \frac{L_j}{d_j} + \sum_k \zeta_{k,j})$ the matrix formulation of the momentum equation is obtained:

$$\mathbf{A}^T \cdot \mathbf{P} = \mathbf{R} \cdot \mathbf{G} - \mathbf{t} \ , \tag{20}$$

where $\mathbf{P}$ is a column vector with dimension equal to the number of nodes which identifies the value of total pressure at each node, $\mathbf{t}$ identifies for each branch the pressure rise due to the pumps. Deriving $\mathbf{G}$ from (20) and defining hydraulic conductance matrix as $\mathbf{Y} = \mathbf{R}^{-1}$:

$$\mathbf{G} = \mathbf{Y} \cdot \mathbf{A}^T \cdot \mathbf{P} + \mathbf{Y} \cdot \mathbf{t} \ . \tag{21}$$

In **unsteady state** condition from equation (14), applying Backward Euler and with constant density it is obtained:

$$(P_{i-1} - P_i)^t = R_j^t \cdot G_j^t + B_j^t \cdot G_j^t - \Delta P_{pump,j}^t - X_j^t \ , \tag{22}$$

where $B_j^t = \frac{L_j S_j}{\Delta t}$ and $X_j^t = -\rho^t \frac{L_j S_j}{\Delta t}\frac{G_j^{t-\Delta t}}{\rho^{t-\Delta t}}$. Now matrix formulation is applied, with $\mathbf{Y'} = \mathbf{R}^t + \mathbf{B}^t$ and the mass flow rate is derived from the equation:

$$\mathbf{G}^t = \mathbf{Y'}^t \cdot \mathbf{A}^T \cdot \mathbf{P}^t + \mathbf{Y'}^t \cdot \mathbf{t}^t + \mathbf{Y'}^t \cdot \mathbf{X}^t \tag{23}$$

The problem with equations (21) and (23) is that matrix $\mathbf{Y}$ is a function of the mass flow rate, which is the unknown. Moreover the pressure is not known. In order to solve this non-linearity the iterative SIMPLE algorithm must be used.

2.2.2 SIMPLE algorithm

The SIMPLE (Semi-Implicit Method for Pressure Linked Equation) [9] algorithm is based on a guess and correction method, and the procedure to be followed is:

1. Guess the pressure vector, that is identified as $\mathbf{P}^*$ and the under-relaxation factors for pressure α_P and mass flow rate α_G. The optimal values of these two number are unfortunately strongly dependent on the typology of network considered.

2. Calculation of $\mathbf{G}^*$ with *fixed-point method*, which is an iterative process needed due to the non-linearity of equation (21). It allows to calculate $\mathbf{G}^*$ thanks to its value at the previous iteration:

$$\mathbf{G}^*_{k+1} = \mathbf{Y}(\mathbf{G}^*_x) \cdot \mathbf{A}^T \cdot \mathbf{P}^* + \mathbf{Y}(\mathbf{G}^*_x) \cdot \mathbf{t} \ , \tag{24}$$

   where, in order to avoid divergence,

$$\mathbf{G}^*_x = a_1 \mathbf{G}^*_k + a_2 \mathbf{G}^*_{k-1} \ , \tag{25}$$

   with $a_1 + a_2 = 1$.

3. Correction of mass flow rate and pressure:

$$\mathbf{G}_{corr} = \mathbf{G} - \mathbf{G}^* \tag{26}$$

$$\mathbf{P}_{corr} = \mathbf{P} - \mathbf{P}^* \tag{27}$$

   By substitution of the two previous equations in (21), after the approximation of $\mathbf{Y}$ with $\mathbf{Y}^*$, it is obtained:

$$\mathbf{G}_{corr} = \mathbf{Y}^* \cdot \mathbf{A}^T \cdot (\mathbf{P} - \mathbf{P}^*) = \mathbf{Y}^* \cdot \mathbf{A}^T \cdot \mathbf{P}_{corr} \ . \tag{28}$$

4. Calculation of matrices $\mathbf{H}$ and $\mathbf{b}$, derived as follows: from equation (10) and (26) it is obtained

$$\mathbf{A} \cdot \mathbf{Y}^* \cdot \mathbf{A}^T \cdot \mathbf{P}_{corr} = -\mathbf{A} \cdot \mathbf{G}^* - \mathbf{G}_{ext} \ , \tag{29}$$

and, consequently

$$\mathbf{H} \cdot \mathbf{P}_{corr} = \mathbf{b} \ , \tag{30}$$

where the above mentioned matrices are defined as $\mathbf{H} = \mathbf{A} \cdot \mathbf{Y}^* \cdot \mathbf{A}^T$ and $\mathbf{b} = -\mathbf{A} \cdot \mathbf{G}^* - \mathbf{G}_{ext}$.

5. Setting of boundary conditions of fluid-dynamic problem, that are about mass flow rate and pressure:

   - Exiting or entering mass flow rate are imposed simply defining the vector $\mathbf{G}_{ext}$, as explained in section 2.2.1.
   - In order to impose pressure at the nodes, it is necessary, at first, set to the i-th element (corresponding to the i-th node) of $\mathbf{P}^*$ at the desired value, and then to modify at every iteration $\mathbf{H}$ and $\mathbf{b}$ in such a way that the i-th element of $\mathbf{P}_{corr}$ is null. To do that, the i-th row of $\mathbf{H}$ must be composed of null elements except for i-th one, that must be set to a value different from zero, while i-th element of vector $\mathbf{b}$ must be zero.

2.2.3 Thermal numerical problem

The solution of this problem is needed in order to analyse the behaviour of the temperature at each node. For this purpose the energy equation (6) is applied to all the nodes of the network. The control volume considered includes the junction, node and half of the pipe linked to the junction (see figure 1), and when the different streams gather into the node, adiabatic and perfect mixing is assumed, and heat losses are ascribed to the branches.

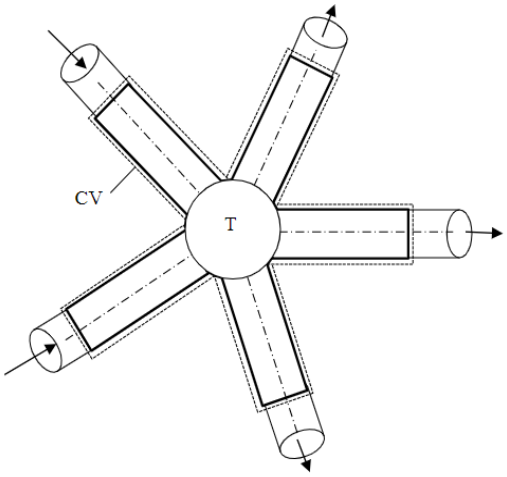

Figure 1: Control volume taken into account [12]

After integration of equation (6) over the control volume above mentioned (reminder: index i refers to nodes, index j refers to branches):

$$\frac{\partial(\rho c_p T_i)}{\partial t} V_i + \sum_j c_p G_j T_j = k \left(\frac{\partial T}{\partial x} \right)_j \cdot S_j + Q_v - Q_l \ , \tag{31}$$

where the control volume $V_i = \sum_{j=1}^{NB} \frac{S_j \cdot L_j}{2}$. Now some simplifications will be applied to the energy conservation equation:

- The conductive term is usually small, so will be neglected;
- The internal heat generation will be considered null;
- Only in a first moment steady-state conditions will be taken into account, thus also first term will be canceled.

The resulting equation is:

$$\sum_j c_p G_j \cdot T_j = -\sum_j \frac{L_j}{2} I_j U_j \cdot (T_i - T_g) \ , \tag{32}$$

where the right side is the expression of heat losses Q_l, with I_j perimeter of the duct j perpendicular to the water flow, U_j the heat transmission coefficient of branch j and T_g the temperature of the ground. The length is divided by 2 because only half of the length of the branches is considered, as already explained.

The equation (32) is now applied to the node i in figure 2. In order to do that it is necessary to apply an appropriate scheme that evaluates the temperatures at the boundary of the control volume (T_j), since temperatures are defined only at the node. For this purpose *upwind scheme* is adopted, this means that the value of the temperature at the boundary is assumed equal to the temperature of upstream node. The upwind scheme has two important properties: it is unconditionally bounded and it takes into account the flow direction so the transportiveness of the mesh is guaranteed. The problem is that this method is first order accurate so numerical diffusion can be present.

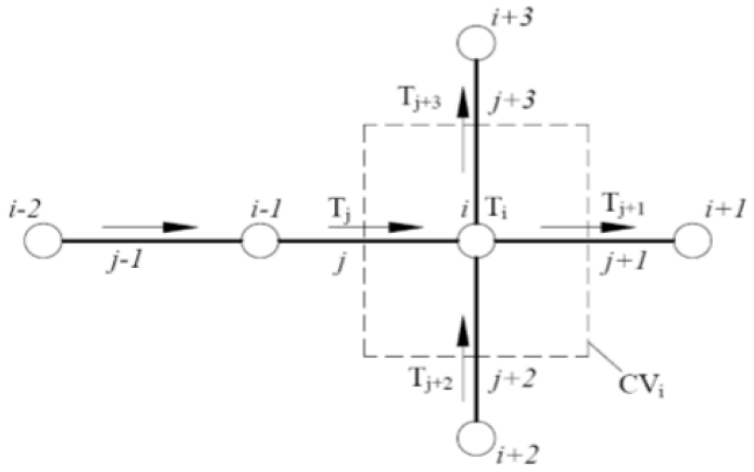

Figure 2: Specific control volume taken into account for equation (33) [12]

$$c_p(G_{j+1} + G_{j+3}) \cdot T_i - c_p G_j T_{i-1} - c_p G_{j+2} T_{i+2} = -(\sum_j \frac{L_j}{2} I_j U_j) \cdot (T_i - T_g) \ , \quad (33)$$

where

$$\sum_j L_j I_j U_j = L_j I_j U_j + L_{j+1} I_{j+1} U_{j+1} + L_{j+2} I_{j+2} U_{j+2} + L_{j+3} I_{j+3} U_{j+3}. \tag{34}$$

Now the temperature terms are gathered:

$$[c_p(G_{j+1} + G_{j+3} + \sum_j \frac{L_j}{2} I_j U_j)] \cdot T_i - [c_p G_{j-1}] \cdot T_{i-1} - [c_p G_{j+2}] \cdot T_{i+2} = (\sum_j \frac{L_j}{2} I_j U_j) \cdot T_g \tag{35}$$

It is now possible to build the *stiffness matrix* $\mathbf{K}$, a square matrix of dimension nxn with n number of nodes in the network. The element $k_{m,p}$ identifies the coefficient of temperature T_p at the node m. After defining $\mathbf{T}$ as the column vector whose elements are the temperature at the nodes and $\mathbf{f}$ the column vector of known terms, the equation (35) can be written in matrix formulation:

$$\mathbf{K} \cdot \mathbf{T} = \mathbf{f} \,. \tag{36}$$

In order to solve the problem it is necessary to impose the boundary conditions:

- INPUT NODES

  It is necessary to set a condition of imposed temperature (*Dirichlet* boundary condition), i.e. setting a value of temperature at the input node, let us call it node m. In order to do that, all the element of the m-th row of matrix $\mathbf{K}$ should be set equal to zero, except the m-th element ($k_{m,m}$) that should be set equal to 1. After that, the value of m-eh element of vector $\mathbf{f}$ must correspond to the temperature desired.

- OUTPUT NODES

  Here a condition of imposed flux (*Robin* boundary condition) is required. More precisely, the thermal losses of the fluid flowing in the branch that precedes the output node (i.e. between the two nodes) are set equal to the thermal losses

of that branch to the environment. The control volume taken into account for this operation is in figure 3. Thus, the energy conservation equation is applied

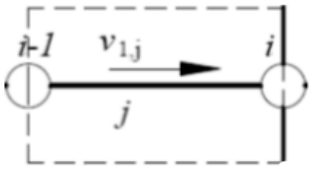

Figure 3: Control volume taken into account [12]

to the output node i, and j is the previous branch, as in figure 3.

$$c_p G_i \cdot (T_{i-1} - T_i) = L_j I_j U_j \cdot (T_j - T_g) \ , \tag{37}$$

where T_j is not defined because temperature is defined only at the nodes, so:

$$T_j = \frac{T_{i-1} + T_i}{2} \ . \tag{38}$$

Please notice that if the output branch is too long, this approximation may bring to numerical diffusion. In order to solve this problem, it is necessary to increase the number of computational nodes ore add a fictitious and sufficiently small output branch.

In the case of **unsteady state** condition, as already mentioned in section 2.2.1, Backward Euler is used to discretize in time, thus equation (31) becomes:

$$\frac{(\rho c_p T_i)^t - (\rho c_p T_i)^{t-\Delta t}}{\Delta t} \cdot \sum_j \frac{S_j L_j}{2} + \sum_j c_p G_j^t T_j^t = -\sum_j \frac{L_j}{2} I_j U_j \cdot (T_i^t - T_g) \ , \tag{39}$$

and, after applying to control volume in figure 2 and gathering according to tem-

peratures:

$$\left[\frac{\rho c_p}{2\Delta t}\cdot(\sum_j S_j L_j)+c_p\cdot(G^t_{j+1}+g^t_{j+3})+\sum_j\frac{L_j}{2}I_jU_j\right]\cdot T^t_i+[-c_pG^t_j]\cdot T^t_{i-1}+ \\ +[-c_pG^t_{j+2}]\cdot T^t_{i+2}=(\sum_j\frac{L_j}{2}I_jU_j)\cdot T_g+\frac{\rho c_p}{2\Delta t}\cdot(\sum_j S_jL_j)\cdot T_i^{t-\Delta t}\ . \tag{40}$$

This can be expressed in matrix formulation, as in steady-state case:

$$(\mathbf{K}+\mathbf{C})\cdot\mathbf{T}^t=\mathbf{f}+\mathbf{C}\cdot\mathbf{T}^{t-\Delta t}\ . \tag{41}$$

At this point, the boundary condition of input nodes is unchanged, while at the output node equation (37), by applying always Backward Euler, becomes:

$$\left[\frac{\rho c_p}{2\Delta t}S_jL_j+c_pG_j+\frac{L_jI_jU_j}{2}\right]\cdot T^t_i+\left[\frac{\rho c_p}{2\Delta t}S_jL_j-c_pG_j+\frac{L_jI_jU_j}{2}\right]\cdot T^t_{i-1}= \\ =L_jI_jU_j\cdot T_g+\frac{\rho c_p}{\Delta t}S_jL_j\cdot\frac{T_i^{t-\Delta t}+T_{i-1}^{t-\Delta t}}{2}\ . \tag{42}$$

2.3 Results validation

Once the behaviour of the district heating network can be simulated, it is necessary to verify if the results obtained are realistic. In order to do that, the following fictitious network has been created.

Node 1 is the inlet node and nodes 7, 12 ,13, 14 are outlet nodes, which simulate the users behaviour.

This model, as it has been developed, provides that the mass flow rates exiting from and entering into the network must be known, in order to define vector G_{ext}. This means that a value of mass flow must be estimated for each user. The procedure adopted is the following:

- Define the maximum users thermal demand (table 1);
- Define the nominal temperature drop between the supply and the return of

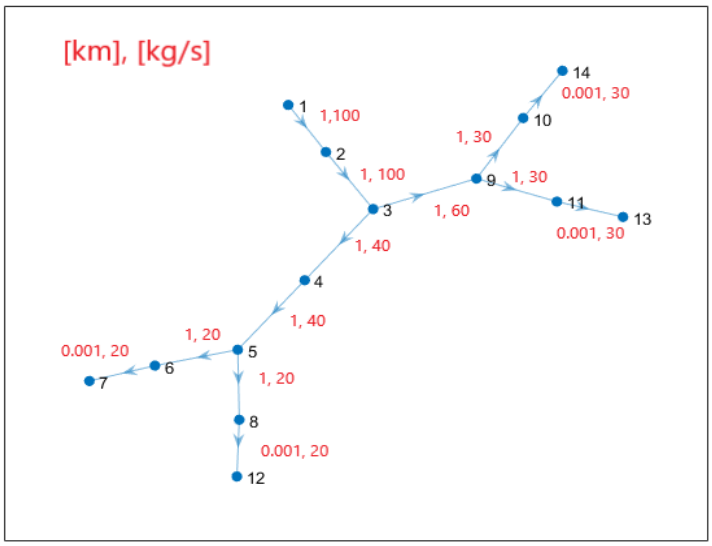

Figure 4: Network taken as an example

district heating network [9]: $\Delta T = 55°C$;

- From the definition of thermal demand

$$\Phi = G \cdot c_p \cdot \Delta T \tag{43}$$

extract the value of mass flow rate to be written in vector G_{ext}.

Table 1: Maximum thermal demand of the users

Node	**[MW]**	**G[kg/s]**
7	5,4	23,89
12	6,5	27,80
13	7,2	32,58
14	7,4	31,27

2.3.1 Mass flow rates

The network taken into consideration has no loops. This means that continuity equation in matrix formulation (10) can be simply solved with Matlab function *mldivide*. In table 2 the results obtained with *mldivide* function and with SIMPLE algorithm are presented, together with the error (in absolute value) of the latter with respect to the former, considered as exact solution.

Table 2: Maximum thermal demand of the users

Branch	$G_{mld}\,[kg/s]$	$G_{SIMPLE}\,[kg/s]$	*Error [%]*
1	115,366	115,537	0,148
2	115,366	115,537	0,148
3	51,874	51,687	0,360
4	51,874	51,687	0,360
5	23,892	23,889	0,010
6	23,892	23,889	0,010
7	27,983	27,798	0,660
8	63,492	63,849	0,563
9	31,731	31,273	1,442
10	32,761	32,576	0,565
11	727,983	27,798	0,660
12	32,761	32,576	0,565
13	31,731	31,273	1,442

It is possible to notice that the errors are small and acceptable for our purposes.

2.3.2 Temperatures

With a network of 14 nodes the temperature obtained at each node are the ones illustrated in figure 5.

This plot shows how the temperature drops from the inlet point until the furthest node. In order to validate these results a space convergence has been performed: increasing the number of nodes for the same district heating network (in figure 4).

The error with respect to the more refined grid is decreasing proportionally with the number of nodes, as the convergence should be. Table 3 shows how increasing

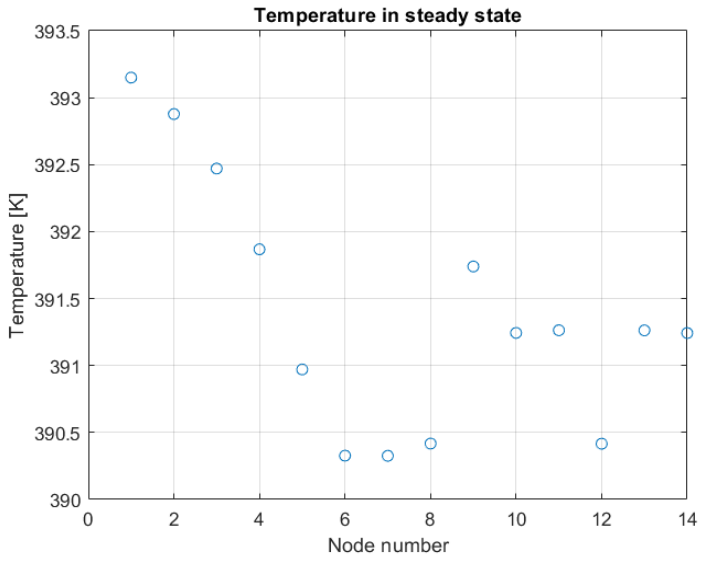

Figure 5: Temperature at each node

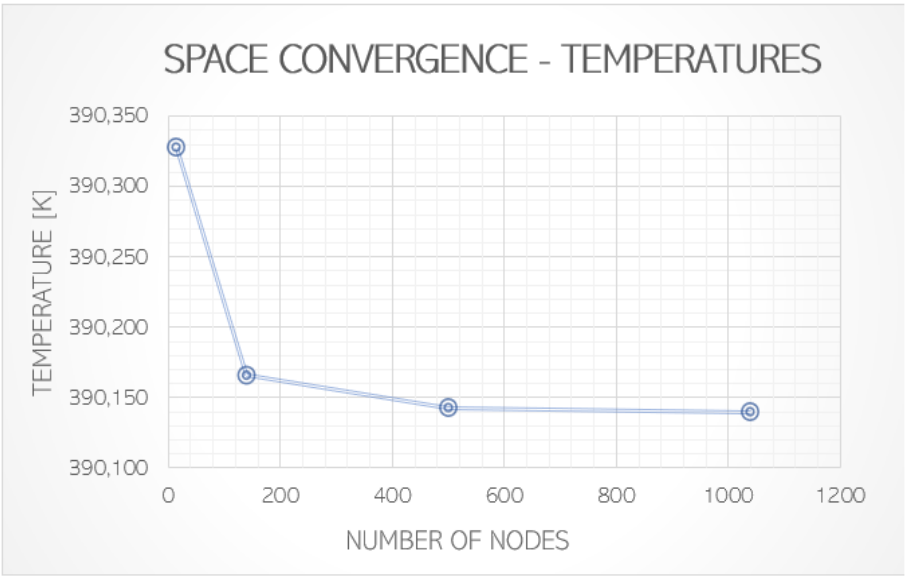

Figure 6: Grid convergence

the number of nodes of the grid the error $R_{i,T}$, calculated in equation (45), decreases.

$$R_{i,T}\,[\%] = \frac{T_i - T_{ref}}{T_{ref}} \cdot 100\ , \tag{44}$$

where T_i is the lowest temperature obtained with the generic grid i, while T_{ref}

is the lowest temperature obtained with the more refined grid.

Table 3: Error of the 3 grids with respect to the more refined one

Number of nodes	Error [%]
14	0,0479
140	0,0067
500	0,0005

On the contrary, in the case of unsteady state condition, the refinement of the grid is more crucial in order to obtain an accurate result. As shown in figure 7, the behaviour of temperature in time (the furthest node has been considered) is described in a different manner according to the grid used. In fact, in a district heating network, the temperature increases in a limited amount of time: at the beginning of the simulation it remains stable, until the hot fluid reaches the node taken into consideration, and then the node reaches in short time the steady state temperature [13]. Obviously, the more refined is the grid the more precise will be the time interval in which the change of temperature occurs. Moreover, you see how the different behaviour between a grid with tens of nodes and a grid with hundreds of nodes is far more remarkable than the different behaviour observed between the two grid with hundreds and thousands number of nodes.

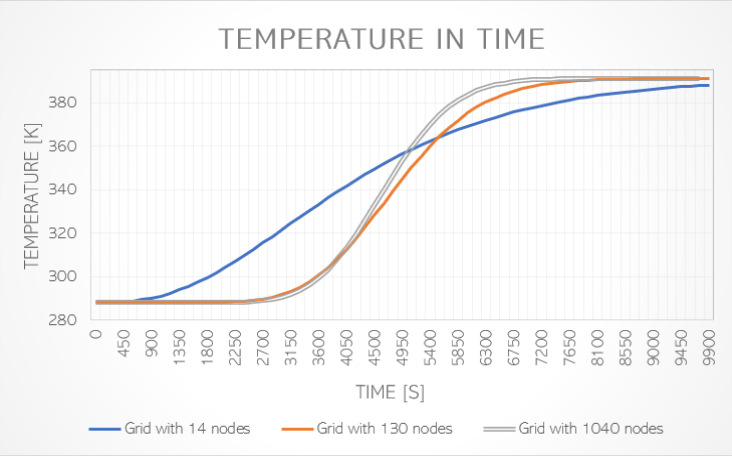

Figure 7: Temperature of the last node in time with three different grid refinements

2.3.3 Pressure drop

Always on the same network in figure 4 the pressure at each node has been calculated with the SIMPLE algorithm, described in section 2.2.2. A pressure of 6 *bar* has been set on the first node, thus pressure drop brings to the results of figure 8. No pumps are considered in the network.

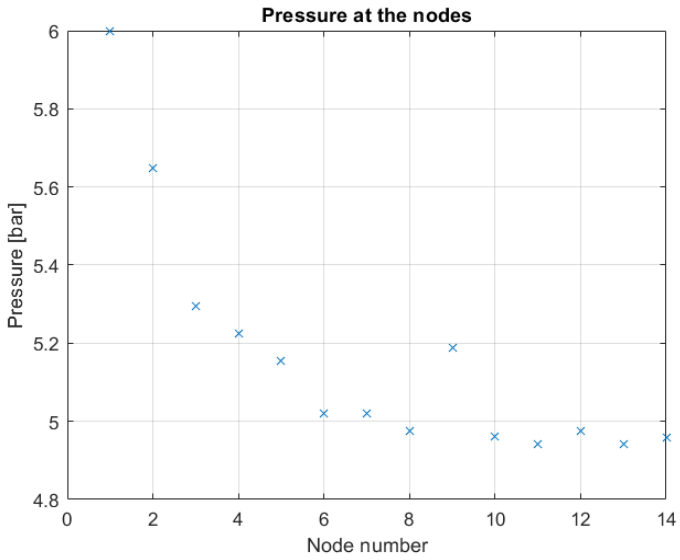

Figure 8: Pressure value at each node

As already done in the case of temperature, a space convergence analysis has been performed to verify the results. Like before, the node with the lowest pressure has been taken as reference, and it turned out to be node 11. This value was extracted for each different refinement of the grid. After this procedure, the plot in figure 9 was obtained.

The error with respect to the more refined grid is decreasing proportionally with the number of nodes, as the convergence should be. Table 4 shows how increasing the number of nodes of the grid the error $R_{i,P}$, calculated in equation (45), decreases;

$$R_{i,P}\,[\%] = \frac{P_i - P_{ref}}{P_{ref}} \cdot 100\ , \tag{45}$$

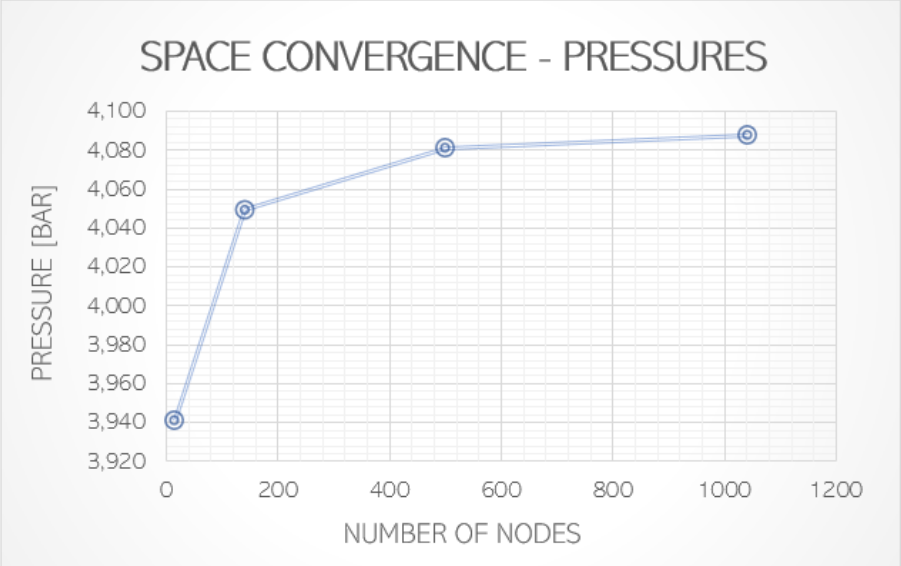

Figure 9: Grid convergence for pressure

where P_i is the lowest pressure obtained with the generic grid i, while P_{ref} is the lowest pressure obtained with the more refined grid.

Table 4: Error of the 3 grids with respect to the more refined one

Number of nodes	**Error [%]**
14	3,595
140	0,938
500	0,165

In order to further validate the results, the residuals of SIMPLE algorithm are attached. Two different type of residuals have been calculated:

- The residual linked to the momentum equation:

$$res_{mom} = max(|\mathbf{Y}^* \cdot \mathbf{A}^T \cdot \mathbf{P}^* - \mathbf{G}^*|) \tag{46}$$

- The residual linked to the continuity equation:

$$res_{con} = max(|\mathbf{A} \cdot \mathbf{G} + \mathbf{G}_{ext}|) \tag{47}$$

For each iteration of the SIMPLE algorithm these two operations have been performed such that the following plots are obtained:

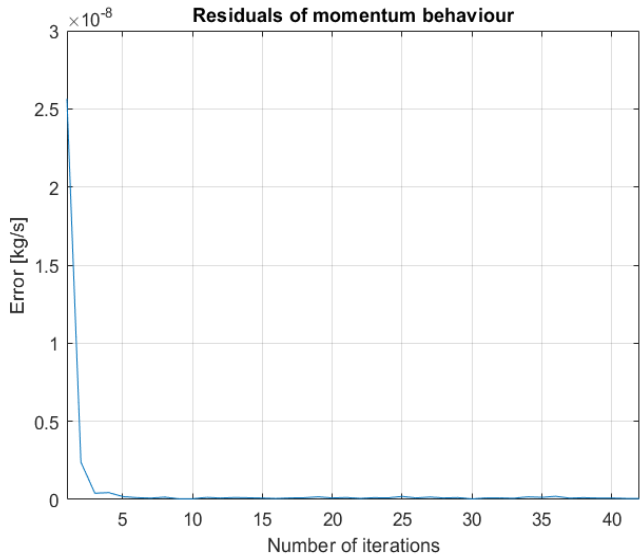

Figure 10: Residual linked to the momentum equation

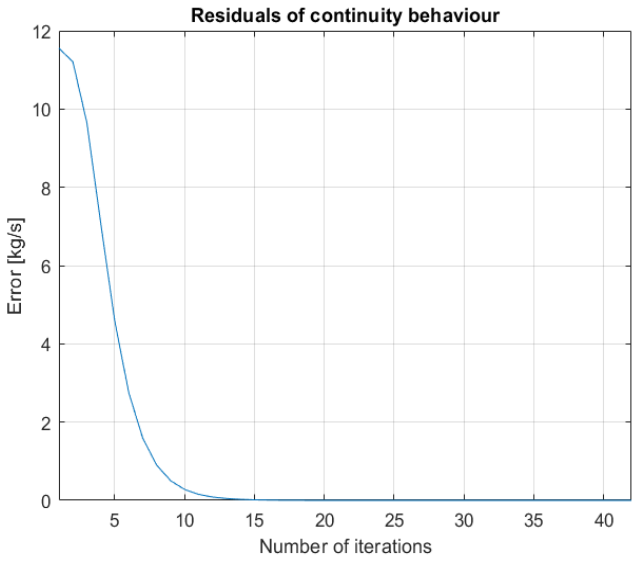

Figure 11: Residual linked to the continuity equation

It can be noticed how both of the residuals converge after about 10-20 iterations of the SIMPLE algorithm, and the higher of the two (res_{con}) reaches the tolerance

imposed (10^{-5}) after about 40 iterations.

As a matter of fact, since the network taken into consideration has no loops, the mass flow rate is known and consequently also the vector of the pressures can be calculated explicitly with equation (19). The calculation brings to the results in figure 12.

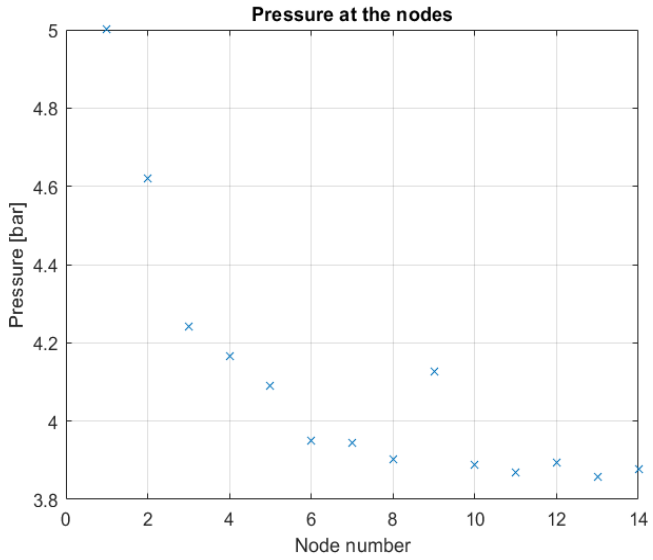

Figure 12: Pressure calculated with momentum equation, without SIMPLE

Thus it is possible to compare these results with the values obtained with SIMPLE algorithm. As table 5 shows, the maximum error occurs in the most distant node and it is around 2%. In practical terms there is a difference between the two models of about 0,025 bar/km.

As final comments, there results are considered satisfactory in order to further analyze the data.

In post-processing some sensitivity analyses will be performed in order to study the fluid-dynamic response of the district heating network to the change of some inputs. Another important parameter that will be fundamental in the final part of the work are heat losses, that in the next section will be mathematically treated.

Moreover the return line behaviour will be simulated and studied, modelling the

Table 5: Percentage error of pressure obtained with SIMPLE with respect to pressure obtained with equation (19)

Node	**Error** [%]
1	0
2	0,578
3	1,260
4	1,411
5	1,568
6	1,769
7	1,919
8	1,844
9	1,493
1	1,839
11	1,870
12	2,049
13	2,154
14	2,099

system according to the real design of actual technologies, that can be found in district heating network spread all over the world.

3 Analysis on the network

3.1 Return network

In order to study the system completely, a model of return network is needed. The work above depicted is useful to simulate the temperature of the transfer fluid that arrives at the users ($T_{out,s}$). At this point the water enters in the heat exchanger in order to provide the requested thermal load to the users, as described in figure 13. At this point, in order to calculate the inlet temperature of return line ($T_{in,r}$) it is necessary to refer to the users heat demand listed in table 1 and, for each user node, the following formula is applied:

$$T_{in,r} = T_{out,s} - \frac{\Phi}{|Gc_p|} \tag{48}$$

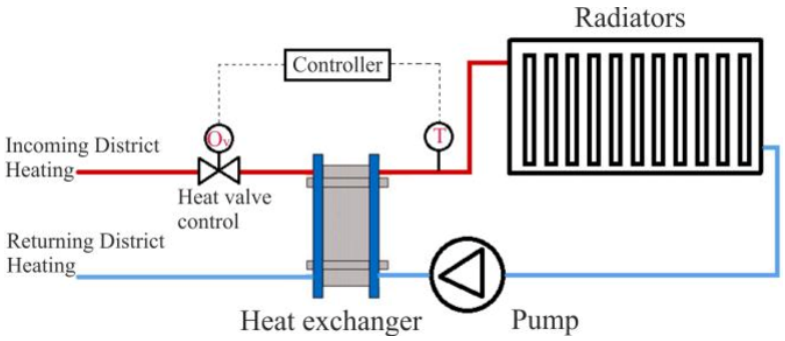

Figure 13: Heat exchanger from district heating to the users [14]

The temperatures obtained are presented in figure 14. The return temperature is about 60°C.

The pressure calculation has been performed with a minimum pressure drop available at the user equal to 2 bar. In this way, in order to obtain the inlet pressure of the return network you just need to subtract the minimum pressure drop available at the user to the outlet pressure of the supply network. The results are in figure 15.

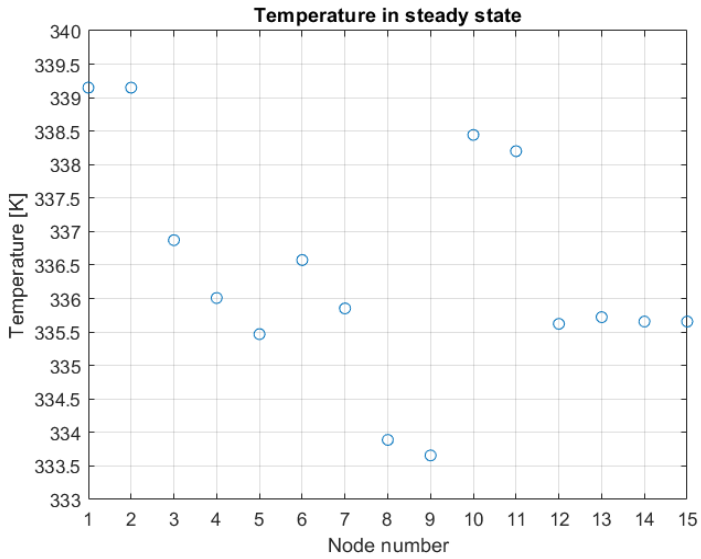

Figure 14: Temperature at each node

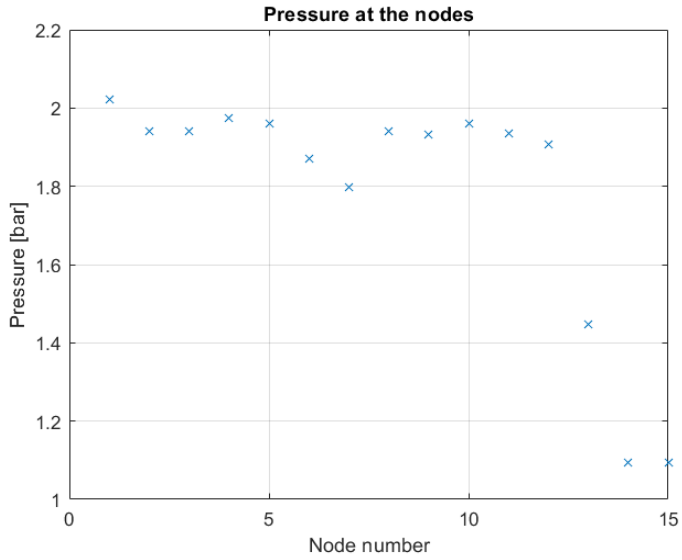

Figure 15: Pressure at each node

At the user it is necessary a pressure of almost 2 bar. This underlines the need of pumps to increase pressure along the network.

3.2 Load variation analysis

In order to study the behaviour of the system in case of load variation, a variation of heat demand by the users has been assumed. This causes, as explained in equation (43), a change of mass flow rate, since specific heat and temperature difference are constant.

In the following plot the data of table 1 have been scaled according to a certain factor (1,25; 1,5; 2), and the temperatures have been calculated again.

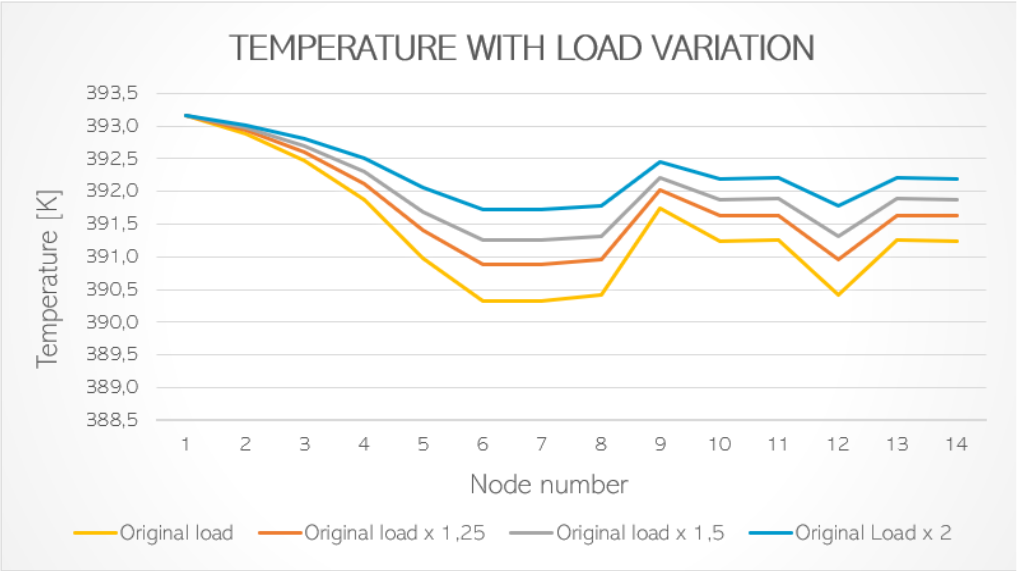

Figure 16: Temperature profile at each node with different heat demand

It can be noticed how, with an increase of heat demand the temperatures are higher. This is because an increase of mass flow rate, being the diameter constant, means an increase of velocity. In this way the hot fluid takes less time to arrive to the users, so it has less time to lose its heat. In simple terms, an increase of thermal inertia occurs.

Obviously the pressure drops will be higher, due to the higher mass flow rate: pressure drops are proportional to the square of velocity.

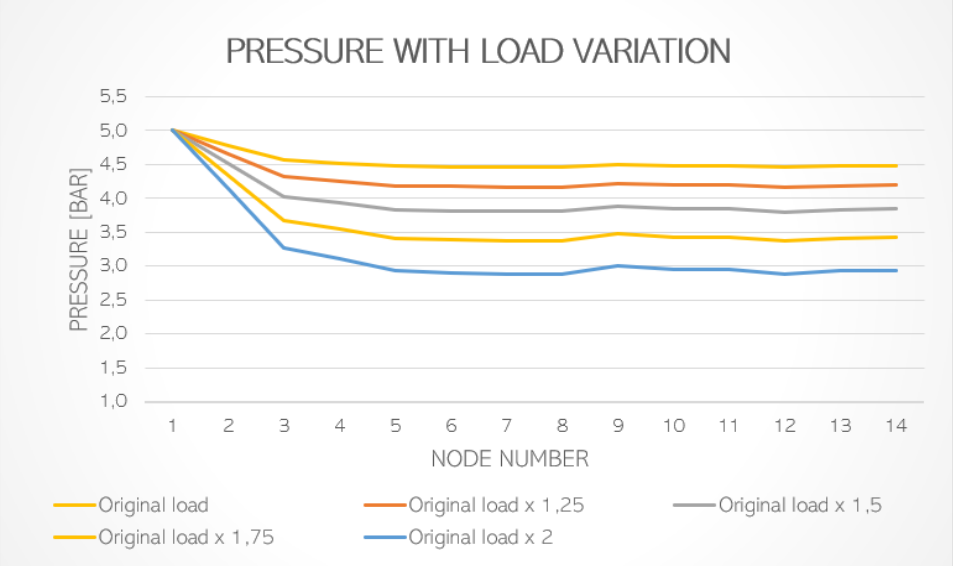

Figure 17: Variation of pressures with the load

3.3 Heat Losses

An analysis of the heat losses in this network taken as example is performed. The value of the heat losses is obtained for generic branch j from the formula, with reference to figure 3.

$$\Phi_{d,j} = \sum_{j=1}^{n_{rami}} L_j I_j U_j \cdot (T_j - T_g) \tag{49}$$

where $T_j = \dfrac{T_i + T_{i-1}}{2}$. This operation is performed for each branch, in this way a profile of heat losses along the network is produced.

3.3.1 Heat losses in steady state

The heat losses are considered in $Watt$, this means that the value of the losses are intended as power lost per second. In the case of temperatures calculated in steady state, in order to calculate the heat losses over a period of time, is obviously necessary to multiply the value in $Watt$ by the time that composes that period.

The code tells us that the values of heat losses in steady state condition are $0,806\,MW$ for the supply line and $0,33\,MW$ for the return line. Obviously the

latter is lower because of the lower temperatures after the heat transfer in district heating substation, as figures 13 and 14 show. The distribution of heat losses for each branch of the two lines is presented in the following plots. The valley in the trend are due to the outlet branches, considerably smaller than the others for the reasons explained in chapter 2.2.3.

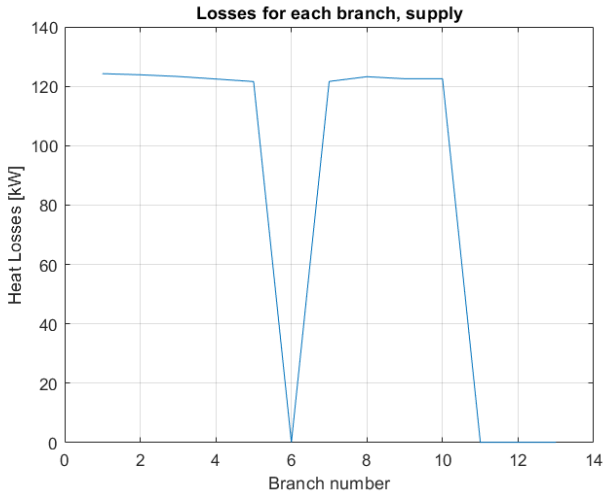

Figure 18: Heat losses for each branch of supply line

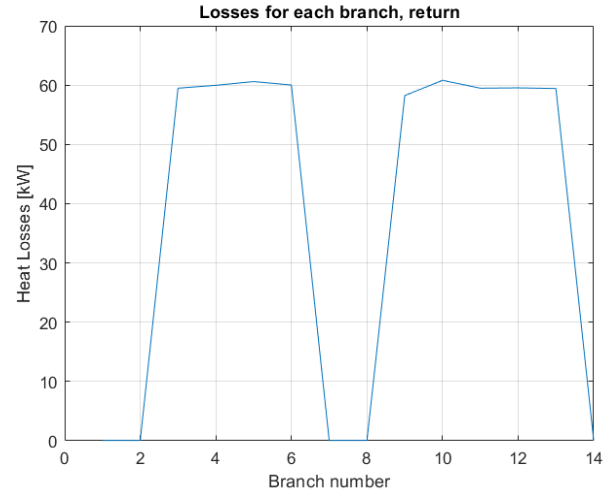

Figure 19: Heat losses for each branch of return line

3.3.2 Heat losses in transient condition

In order to calculate the heat losses while the system is switching on or off, it is necessary to calculate the losses with the temperatures obtained in every time step of unsteady state condition. The sum of them is the total losses during the transient operation.

The trend is expected to be increasing with time, since the temperatures of the network increase with time thanks to the incoming hot fluid. Moreover the trend is not linear because, as figure 7 shows, the temperature at a generic node does not increase linearly.

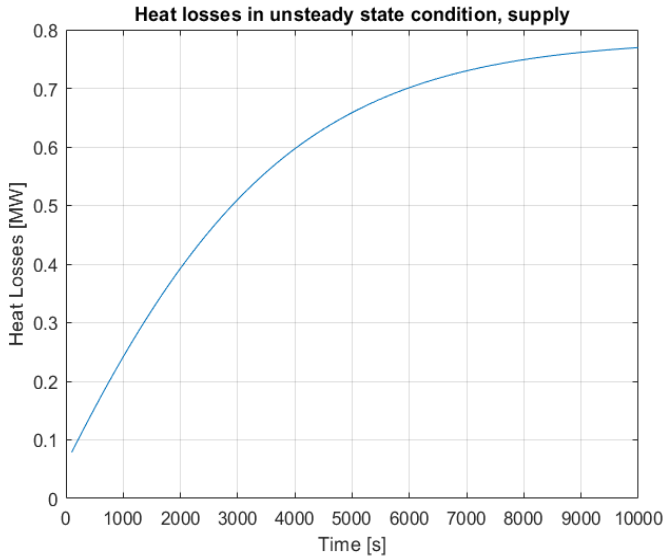

Figure 20: Heat losses in time of supply line

As it can be seen both the transient start after the first time step with a value of losses that is almost equal between the two, since at time 0 they are the same network at the same temperature. After the transient has finished, the final value is equal to the one calculated in steady state condition.

It is possible to notice that the return curve has an almost linear behaviour at first time, this is due to the initial temperature which is really close to ground temperature, and so the increasing trend is faster and almost linear.

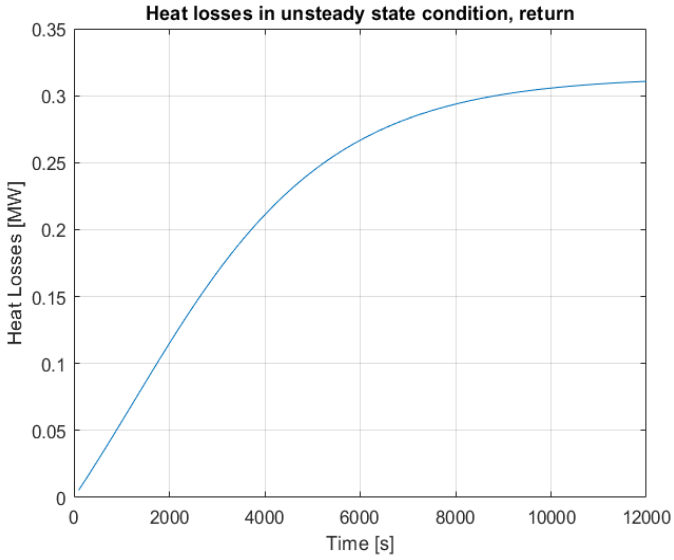

Figure 21: Heat losses in time of return line

3.3.3 Sensitivity analysis with ground temperature

Heat losses will be an important parameter to evaluate the systems in next chapters, for this reason a further confirmation of the results is deemed to be necessary.

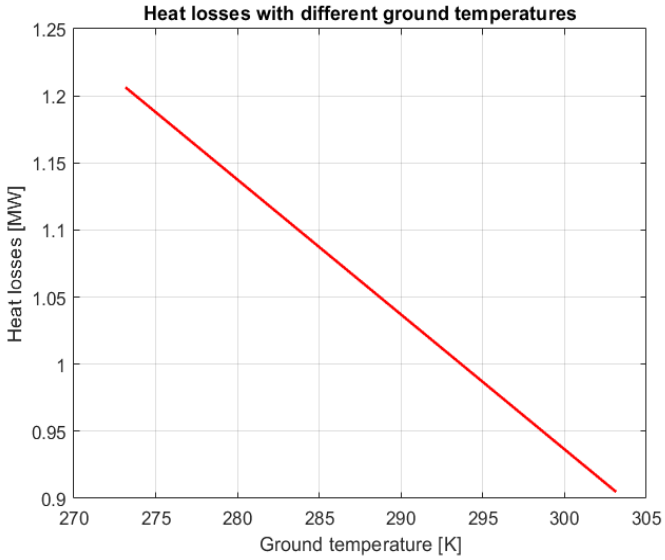

Figure 22: Heat losses dependent on ground temperature

As equation (49) shows, being constant the coefficients, the value of heat losses

are linearly proportional to ground temperature: the more it is higher, the lower will be the dissipation of heat toward the environment. The plot in figure 22 corroborates this analysis.

4 Case study: introduction of district heating in a gas network

In order to apply the model constructed and described in the previous chapter, a substitution of natural gas users with district heating users in a industrial and urban area is taken into consideration.

4.1 Urban area description

The urban area concerned is described in the figure 23.

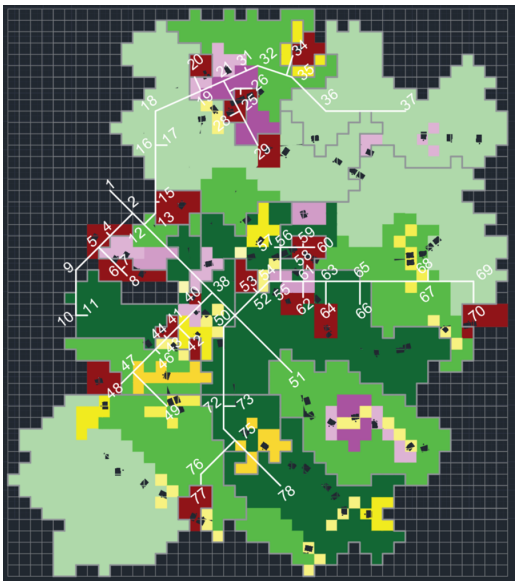

Figure 23: Urban area topology

The unit cell dimension is 100 x 100 m, while the entire square is 4.4 x 5 km. Different colours correspond to different kind of users:

- Green: RESIDENTIAL user. Different shade: low-medium-high density (from light to dark).
- Yellow: COMMERCIAL user. Different shade: electricity meter allowed power (6, 10, 15, 20 and 30 kW from light to dark).

- Pink: OFFICES. Different shade: electricity meter allowed power (3, 6 and 9 kW from light to dark).
- Red: INDUSTRIAL user.

As far as the natural gas flow rate is concerned, the figure 24 describes the area.

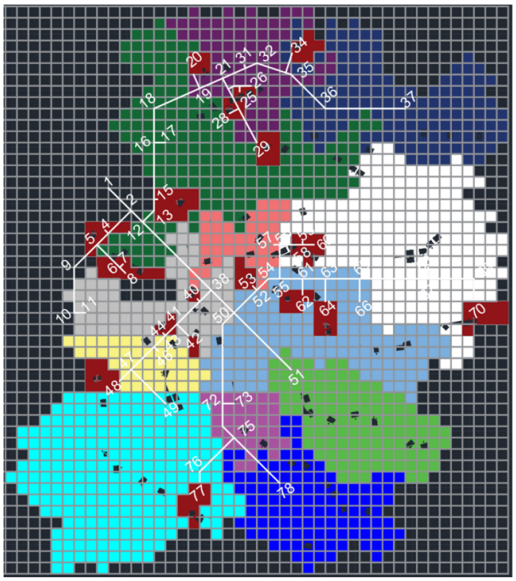

Figure 24: Natural gas volumetric flow rate

Each zone is fed by second jump reduction group in which the pressure drops down, so that it can supply a low pressure network until the gas meter of each user. The area coloured in dark red are industrial area directly fed by medium pressure network. The other colours identify the maximum hourly volumetric flow rate of natural gas, according to the legend of figure 25.

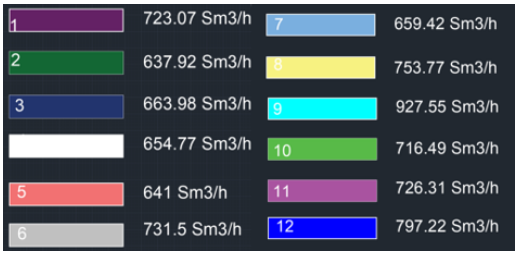

Figure 25: Legend of natural gas flow rate

For the sake of clarity, the following table shows the consumption of natural gas for each node.

Node	NG [Sm^3/year]	*Node*	NG [Sm^3/year]
4	1931580	*46*	239096
7	1724625	*48*	2207520
8	1379700	*49*	912016
11	730075	*51*	1359881
15	3035340	*53*	1724625
17	1285516	*57*	527677
20	1379700	*59*	1379700
25	1241730	*60*	1034775
26	413910	*62*	1724625
28	827820	*64*	1655640
29	1655640	*66*	1429572
31	1534440	*68*	1147433
34	1655640	*70*	2207520
37	686383	*73*	266556
40	413910	*77*	2207520
42	827820	*78*	919732
44	1034775	*1 (TOT)*	42702493

Figure 26: Natural gas consumption for each node

Before moving to the system sizing, a specification is necessary. What in figures 23 and 24 is represented as a node, is not a single user but a group of users. The figure 27 sums up the topology in detail.

	RESIDENTIAL		OFFICES		COMMERCIAL	
Node	*Users*	*[Sm^3/year]*	*Users*	*[Sm^3/year]*	*Users*	*[Sm^3/year]*
11	281	531701	90	134346	33	64028
17	385	728535	270	537383	12	19598
31	172	325329	450	1209111	0	0
37	203	383061	180	268691	11	34631
46	88	165622	0	0	23	73474
49	428	808793	0	0	47	103224
51	272	514611	360	806074	24	39196
57	103	194957	180	268691	33	64028
66	614	1160881	90	268691	0	0
68	439	829746	90	268691	24	48995
73	112	212680	0	0	11	53876
78	450	850853	0	0	33	68880
TOT	3547,2	6706769	1709,8	3761679,6	249,6	569929,3

Figure 27: Users of the network

4.2 Consumption profiling

4.2.1 Daily consumption

In figure 26 are listed the users heat demands for each node of the network. Before starting with the simulation it is necessary to translate the total annual consumption in hourly consumption, in order to obtain the water mass flow rate needed as an input of the Matlab code.

In order to do this, an important document of the natural gas authority comes into help [27]. In this document (Section 2, Article 5 and 6) the profiling procedure is described. It consists in taking the annual value and multiplying it by the daily percentage value $p^{\%}_{PROF,k}$. This parameter is different for each day of the year, and it allows to obtain, from the annual consumption, a value of consumption for each day of the year. The calculation is based on other parameters that change according to the season, the month and even the day of the week:

$$p^{\%}_{PROF,k} = W_{kr} \cdot \beta 1_{PROF} \cdot c1^{\%}_{i,j,k} + \beta 2_{PROF} \cdot c2^{\%}_{k} + \beta 3_{PROF} \cdot 1^{\%}_{j,k} + \beta 4_{PROF} \cdot c4^{\%}_{k} \quad (50)$$

where:

- i is the climatic zone (A, B, C, D, E, F)
  E class is chosen, which is the zone of Pianura Padana (including Torino) and central Italy mountains, as shown in figure 28 and 29.
- j is the picking class, defined in table 6.

Table 6: Picking class from arera [27]

CODE	PICKING CLASS
1	7 days
2	6 days (Sunday and festivities excluded)
3	5 days (Saturday, Sunday and festivities excluded)

In this study class 1 has been chosen for industrial and residential users, while

Figure 28: Climate zone in Italy

Climate zone	Degree Day (DD)
A	<600
B	600 - 900
C	901 - 1400
D	1401 - 2100
E	2101 - 3000
F	>3000

Figure 29: Legend of climate zone in Italy and corresponding Degree Day values

class 3 for offices and commercial users.

- $c1^{\%}_{i,j,k}$ is the percentage value in the day k of standard picking connected to the gas used for heating purposes, in climate zone i and for picking class j.
- $c2^{\%}_{k}$ is the percentage value in day k of standard picking connected to food cooking and/or sanitary hot water.
- $t1^{\%}_{j,k}$ is the percentage value, at day k, of standard picking connected to technological use of natural gas and picking class j.
- $c4^{\%}_{k}$ is the percentage value in day k of standard picking connected to the is of gas for conditioning.

- $\beta 1_{PROF}$, $\beta 2_{PROF}$, $\beta 3_{PROF}$, $\beta 4_{PROF}$ are coefficients, defined in table 7, that identify the category of use of gas.
- W_{kr} is a climate correction factor associated to day k and climate region r.

All these values are published in the website of the company that is Balance Responsible (the bigger distribution company).
For this study, category C3 is chosen (heating + cooking and/or production of sanitary hot water). In order not to consider the cooking gas demand in the total demand that district heating must supply, the consumption of residential users has been decreased of a 5%.

Table 7: Gas category of use [27]

CODE	DESCRIPTION
C1	7 Heating
C2	Cooking and/or hot water production
C3	Heating + cooking and/or hot water production
C4	Conditioning
C5	Conditioning + heating
T1	Technological use
T2	Technological use + heating

The calculation in this way performed brings to the results shown in figure 30. The numbers on x-axis are the day of the year, considering 1 as $January\,1^{st}$.
It can be noticed how, considering climate zone E, space heating is active only from October 15^{th} until April 15^{th}.
The maximum daily consumption is reached in mid-January and it consists in 254,024 Sm^3/day of natural gas, while the minimum is obviously reached in summer and it is of 20,737 Sm^3/day.
Those peaks and valleys in heating period are due to the day of the week: in Saturday and Sunday all the offices and commercial users heating are considered to be switched off. For further clarification in figure 31 is specified the natural gas consumption of a generic winter week.

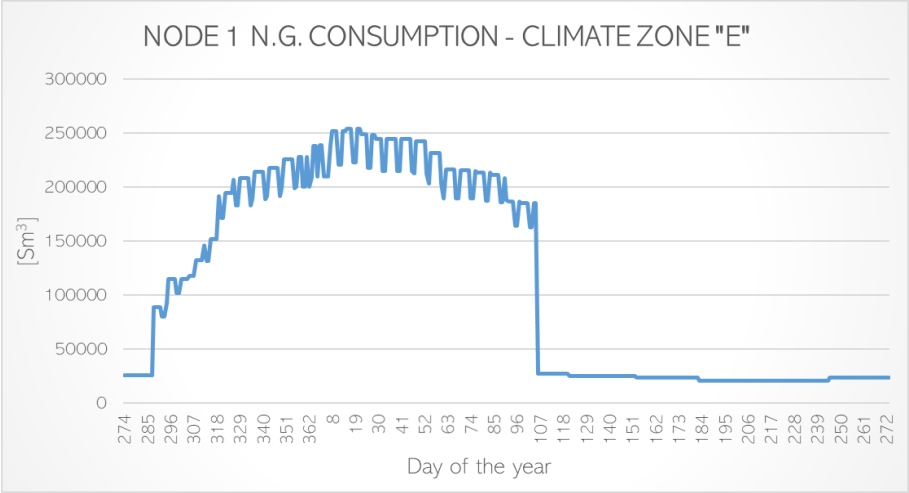

Figure 30: Total annual consumption of the users

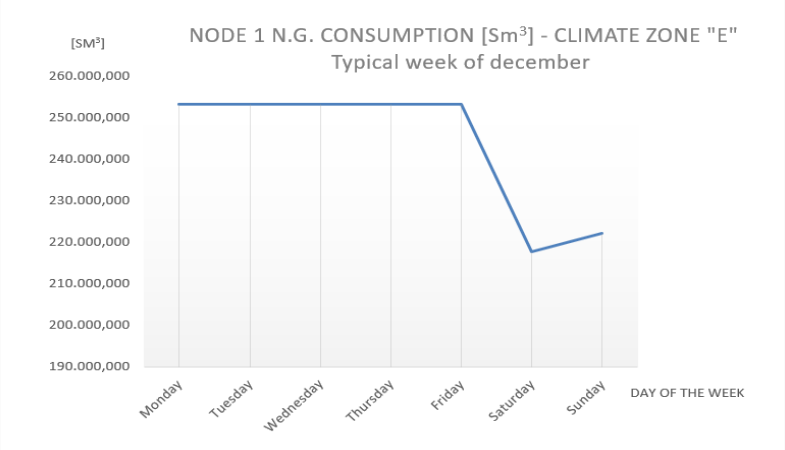

Figure 31: Weekly consumption of the users

4.2.2 Hourly profiling

Now from the daily consumption it is necessary to obtain an hourly profile in order to give the input at the Matlab Code.
The method used is a simple multiplication of the daily value by a percentage $p\%$ that is taken from the figure 32 and that changes according to the time of the day.

From the plots is clear how the residential users and offices have a very low consumption during night, while industries and commercial users have a remarkable activity also during the night.

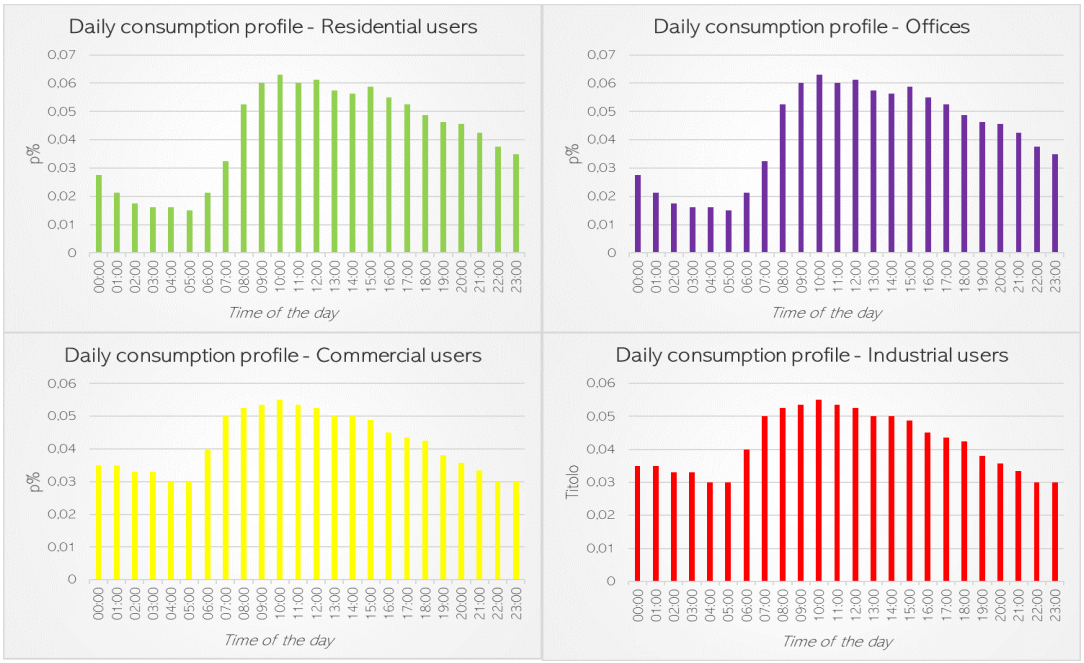

Figure 32: Hourly consumption percentage with respect to total daily consumption

4.2.3 Calculation of thermal demand and mass flow rate

The last step before running the code is calculate the hourly mass flow rate. In order to do that it is necessary to know the heat demand of each user.

The starting point is the natural gas consumption q_{NG}. Imposing a Low Heating Value of natural gas LHV_{NG} of 35.046 $\frac{MJ}{Sm^3}$ [25] and a *nominal* temperature drop between the supply and the return line of DHN:

$$\Delta T_{nom} = (129°C - 65°C) = 55°C \tag{51}$$

it is possible to calculate the thermal power demand from the natural gas consumption q_{NG}:

$$\Phi[W] = q_{NG} \cdot LHV_{NG} \cdot \eta_{th} \ , \tag{52}$$

after that, considering the definition of heat demand:

$$\Phi = G \cdot c_{p,water} \cdot \Delta T \tag{53}$$

from equations (52) and (53) it is possible to calculate the mass flow rate profile for each node:

$$G = \frac{q_{NG} \cdot LHV_{NG} \cdot \eta_{th}}{G \cdot c_{p,water}} \tag{54}$$

At this point all the values needed are known, except for the thermal efficiency of the natural gas boilers. For the estimation of it an important document published by Piemonte comes into help [28]. In the Annex there is the method for the calculation of the *minimum* combustion efficiency allowed, measured at maximum effective thermal power in condition of normal operation, resulting in the following expression:

$$\eta_c\,[\%] = 0.9 \cdot [93 + 2 \cdot log(P_n)] \tag{55}$$

where $log(P_n)$ to base 10 of useful nominal thermal power of the generator. For values $P_n > 400\,kW$, the maximum limit of 400 kW is applied.
Since these are the minimum values that the Authority impose to reach within September 2020, a 90% of this value is supposed.

In the case of this work the efficiency obtained in this way vary from 0.87 and 0.88.

This method allows to calculate also the hourly profile of thermal demand and consequently mass flow rate. The results for node 1 (which means the total of the system) are shown in figure 33, taking into consideration a generic day of February (near the maximum power demand).
It is possible to notice that during the night the demand is not negligible, and it is not less than one half of the peak demand. This leads to think that switching off the district heating during night is not feasible and convenient, but this topic will

be treated more in detail in next chapter.

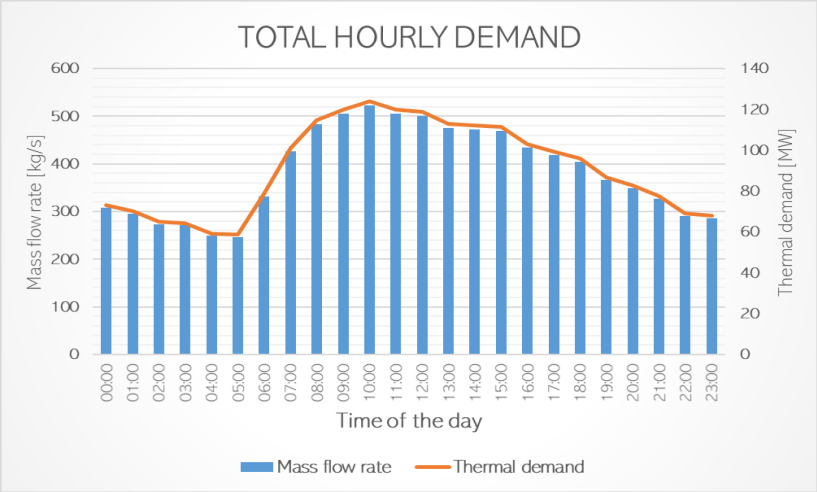

Figure 33: Total hourly power demand and hourly mass flow rate

4.3 Application of case study at the numerical model

At this point the mathematical model implemented in previous chapters is applied to this case study in order to analyze it and build a proper production energy system.

The first thing to decide is the time configuration of district heating network: continuous operation or switching mode (activation in the morning)? For this purpose a transient operation is supposed, described in section 4.3.1.

4.3.1 Switching mode

Under the assumption that during the night the thermal losses bring the system agian to ground temperature, if the district heating is turned on in the morning, a peak of demand happens, because the main plant load is impacted by three factor deriving from users behaviour:

1. Presence of a peak of request from 2 to 5 times higher than the stationary request in the afternoon.

2. Peak of request strengthened by the fact that the thermal load must heat up at the operating temperature a network that is all at ground temperature.

3. Demand variation is linked to a mass flow rate variation that has an immediate effect on plants thermal load (delay of about 0.5 s/km, because fluid-dynamic perturbations travel with sound speed).

4. Request variation is connected to a return temperature variation that has a delayed effect on plant load (considering mean velocity of 1 m/s, the delay is around 15 min/km.

For all these reasons an example of plant thermal load is like the one presented in figure 34. Obviously the values are much higher than the ones treated in this case study because the plot refers to the entire city of Turin.

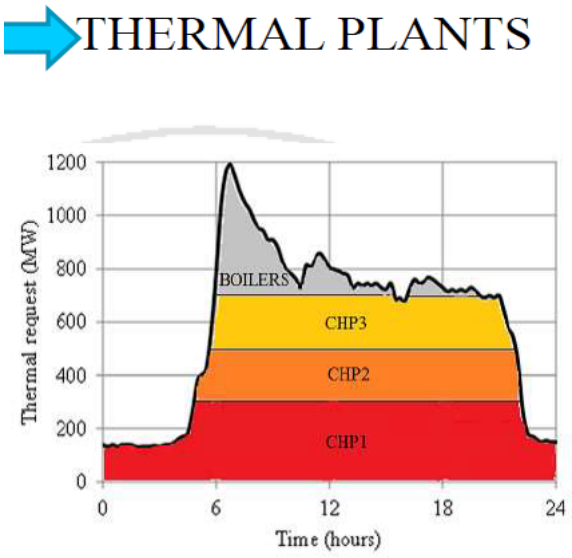

Figure 34: Total plant load in Turin [29]

With the aim of simulating this situation, a guess has been made. There are two ways for simulate the heat demand variation of the user:

1. Primary net mass flow rate variation;

2. Variation of ΔT at the primary net.

In this case ΔT has been considered fixed at $55°C$, because the hypothesis is that once set point temperature at secondary net supply (the temperature which has the water sent directly to the user terminal) is decided, the regulator changes the primary net mass flow rate that enters into the heat exchanger of the substation. Return temperature of primary side (T2 in figure 35) will be function of the temperature of the primary side (T1) and of the value of mass flow rate decided by the regulator.

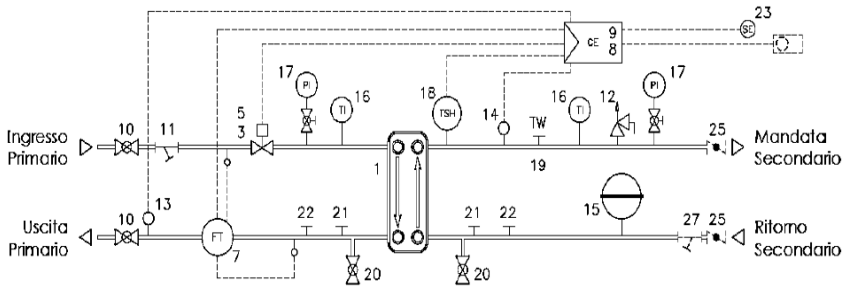

Figure 35: Substation scheme in a district heating network [30]

In order to simulate the switching mode a mass flow rate of about 2 times higher with respect to the stationary demand is supposed, and the data in figure 36 and 37 have been used.

The pipeline diameters are sized in order to avoid velocities higher than $v_{max} = 2,5\, m/s$:

$$D_k = \sqrt{\frac{4 \cdot G_k}{\pi \cdot \rho \cdot v_{max,k}}} \tag{56}$$

where k is the generic branch.

The linear length of the network is $L_{tot} = 15.166\, km$ The study has been done for a *medium value* of mass flow rate of a January day. The coefficient c_m is the coefficient that multiplies the stationary mass flow rate to obtain peak mass flow rate, and it is higher for further nodes that struggle to arrive at temperature.

Moreover, the other input data are:

branch	L (m)	D (mm)	branch	L (m)	D (mm)	branch	L (m)	D (m)
1	283	500	27	90	100	53	141	300
2	283	200	28	10	150	54	100	300
3	4	150	29	219	250	55	300	200
4	141	200	30	30	150	56	50	100
5	283	200	31	109	200	57	200	200
6	40	150	32	267	200	58	30	150
7	70	150	33	180	0,15	59	100	100
8	283	100	34	49	150	60	200	200
9	400	100	35	424	150	61	140	150
10	100	100	36	700	150	62	200	200
11	141	500	37	849	400	63	200	100
12	141	300	38	141	250	64	300	250
13	100	300	39	5	100	65	200	150
14	30	200	40	25	250	66	600	200
15	500	350	41	25	100	67	100	150
16	100	100	42	141	200	68	400	150
17	300	350	43	30	100	69	200	150
18	438	350	44	141	200	70	141	200
19	134	150	45	5	100	71	700	200
20	219	300	46	283	200	72	100	100
21	107	200	47	141	100	73	200	200
22	57	150	48	100	100	74	141	200
23	50	150	49	283	300	75	424	150
24	50	150	50	207	150	76	100	150
25	97	100	51	283	300	77	566	150
26	195	200	52	50	150	-	-	-

Figure 36: Diameters and length of pipelines

NODE	c_m	G_{stat} [kg/s]	G_{peak} [kg/s]	NODE	c_m	G_{staz} [kg/s]	G_{peak} [kg/s]
1	1,65	-395,73	-652,96	44	1,65	9,09	15,00
4	1,65	16,97	28,00	46	2	2,36	4,72
7	1,65	15,15	25,00	48	2	19,40	38,79
8	1,65	12,12	20,00	49	2	8,38	16,76
11	2	7,12	14,24	51	1,65	14,95	24,67
15	1,65	26,67	44,01	53	1,65	15,15	25,00
17	1,65	13,27	21,90	57	1,65	5,82	9,60
20	1,65	12,12	20,00	59	2	12,12	24,25
25	1,65	10,91	18,00	60	2	9,09	18,18
26	1,65	5,11	8,43	62	1,65	15,15	25,00
28	1,65	7,27	12,00	64	2	14,55	29,10
29	1,65	14,55	24,00	66	1,65	13,52	22,30
31	1,65	17,78	29,34	68	2	11,21	22,42
34	2	14,55	29,10	70	2	19,40	38,79
37	2	10,76	21,52	73	2	2,53	5,07
40	1,65	3,64	6,00	77	2	19,40	38,79
42	1,65	7,27	12,00	78	1,65	8,33	13,74

Figure 37: Mass flow rate for each node, with peak mass flow rate

- Roughness ϵ=0.003 mm
- Heat transfer coefficient of the pipes toward the ground h=1.2 $\frac{W}{m \cdot K}$
- Specific eat of water $c_p = 4186 \frac{J}{kg \cdot K}$

- Ground temperature $T_g = (120 + 273.15)\,K$
- Mean water density $\rho_{water} = 970\,\frac{kg}{m^3}$
- Friction factor λ_j calculated like in section 2.2.1.

With all these input data the code can run. The first results are velocities and pressures.

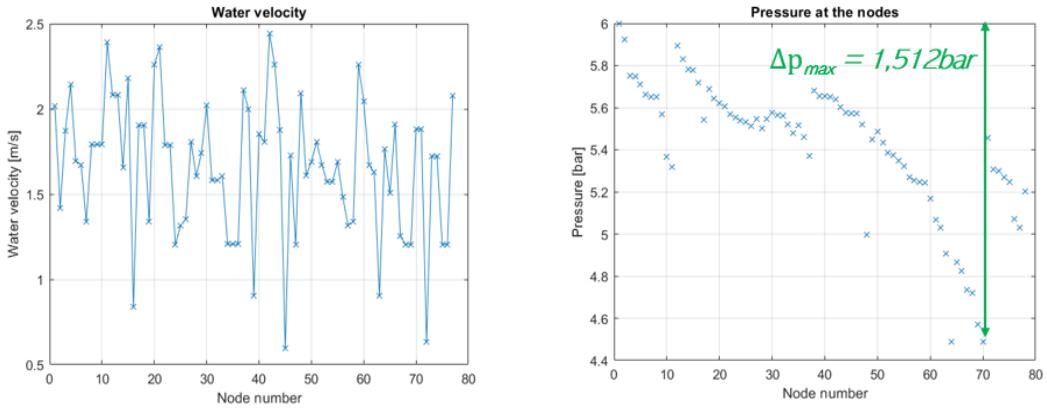

Figure 38: Pressure and velocity of switching mode

The velocity values are stopped at 2.5 m/s, as already explained, while the maximum pressure drop (in supply side) is 1.512 bar, that is a high but affordable value, since the pumping system load would be:

$$t_{PUMP} = \Delta P_{max} + P_{min} + L_{user} = 5.512\,bar \tag{57}$$

where P_{min} is the minimum return pressure to the plant (2 bar) and L_{user} is the pressure drop at the user, supposed to be 2 bar.

As far as heat losses are concerned, both for supply and return line, figure 39 shows as they rapidly increase when the network is near the ground temperature, while it reaches a plateau after about 2 hours.

The thermal power peak, instead, is visible in figure 40, due to the reasons already explained in the previous paragraph.

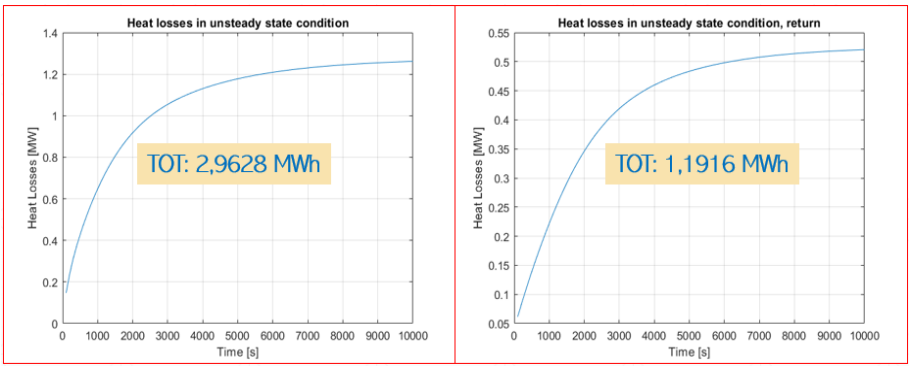

Figure 39: Heat losses in time for supply and return line

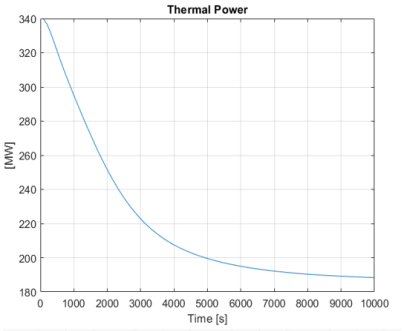

Figure 40: Thermal power in time provided to the network

The real problem of this configuration, though, are the temperature reached in time. In fact, starting from ground temperature in the morning the system must be capable of bringing all the users at the stationary temperature in a proper time. This proper time is supposed equal to 2 hours. But after 2 hours the situation is the one described in figure 41.

The blue line identify the stationary temperature (with a tolerance), and it is possible to notice that not all the nodes have reached that value. In particular, all the users at nodes 11, 26, 34, 37, 68, 70, 73, 77 and 78 have a temperature too low for the correct operations of the substation heat exchanger. Moreover, it would be infeasible to increase velocities, because they are already at the maximum limit, and pressure losses would be too high.

For a better comprehension, the figure 42 shows the graph representation of

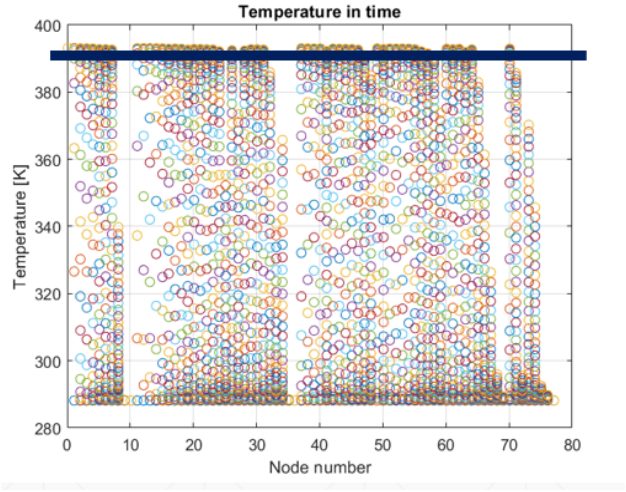

Figure 41: Temperature at the nodes after 2 hours from the switching

the temperature after 2 hours. It can be seen how the furthest node are not in temperature.

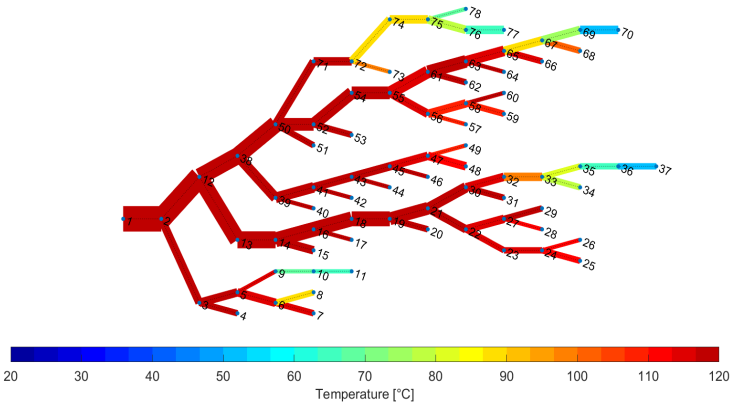

Figure 42: Temperature at the nodes after 2 hours from the switching on

It follows that the switching mode is not the best option in this case, also because the consumption at night is not negligible and it justifies a continuous operation mode for district heating network.

4.3.2 Continuous operation mode

At this point the continuous operation mode is simulated.

In order to do that, from the calculation of hourly consumption the hourly mass flow rate is extracted for each node. The transient model has been performed with a time step of 100 seconds: the value of mass flow rate available has a discretization of 1 hour, so in order to transform the 1 hour step in a 1000 seconds step a linear variation of mass flow rate is supposed. With interpolation the input values for the code every 100 seconds are obtained.

By way of illustration, the steady state temperature for supply and return line, in the case of maximum mass flow rate reached in January are showed in figure 43.

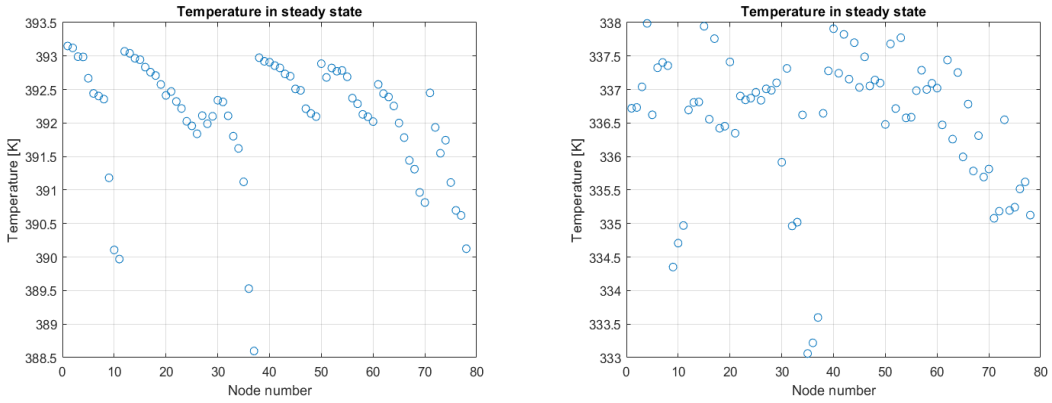

Figure 43: Temperature in steady state of supply and return line

For a better comprehension of the situation in the network, the figures 44 and 45 are proposed, that depict the temperature and velocities of the line. The coloured walls of the branches are referred to the legend at the left of the figure, while the colour in the center of the branches is referred to the legend at the bottom, showing temperature.

Here it is clear how the temperature has a descending trend, more and more as we are far from the feed of the hot water. The velocities instead do not have an organised trend, because they depend on the mass flow rates that are lower so as they are far from the injection, but also on diameters.

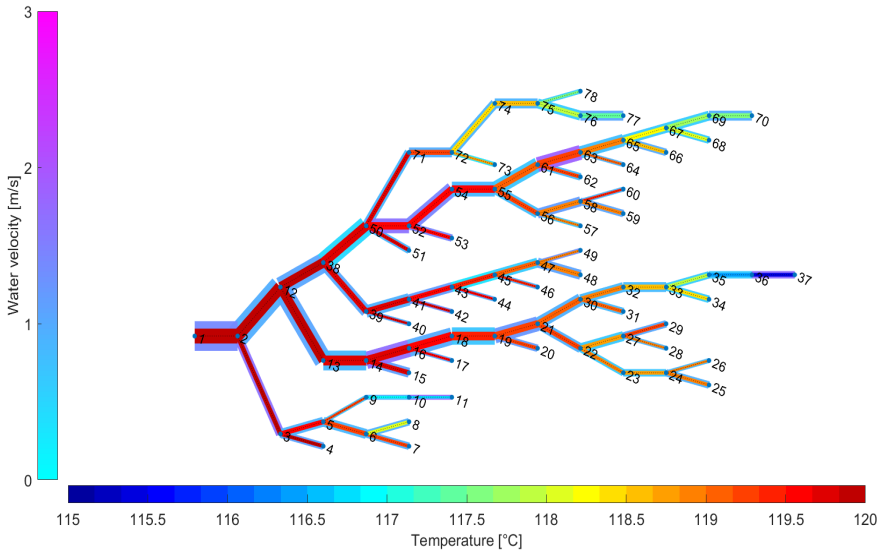

Figure 44: Temperature in steady state and velocities of supply line

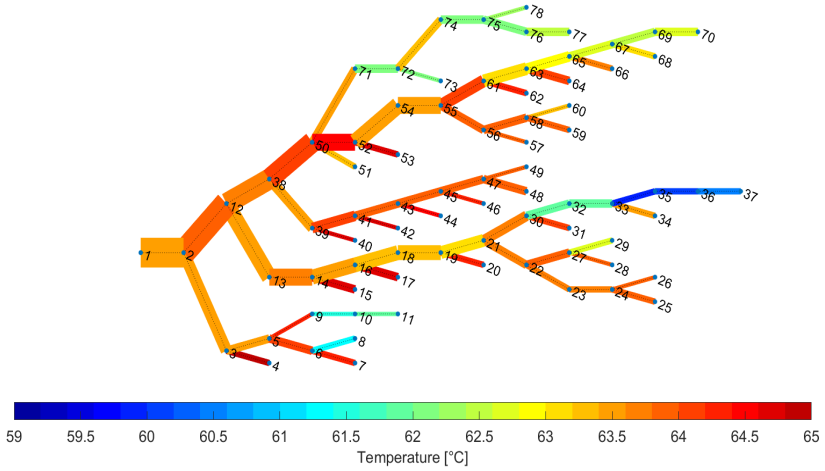

Figure 45: Temperature in steady state of return line

The temperature decreases of about $4.5°C$. The return line has less "organized" temperature because the mass flow rate has inverted sign, so there is not separation of the flows but mixing of the flows. As a matter of fact it can be noticed how one the furthest node of return (node 1) the temperature is higher than the temperature of some nodes that are at the beginning of this return line, near the users.

Always by way of illustration figure 46 describe the heat losses for each branch. It is possible to notice how branch 37 is the longer one of the network, and consequently it dissipates the higher amount of thermal power to the environment. Obviously the return line heat losses are way lower because of lower operating temperature.

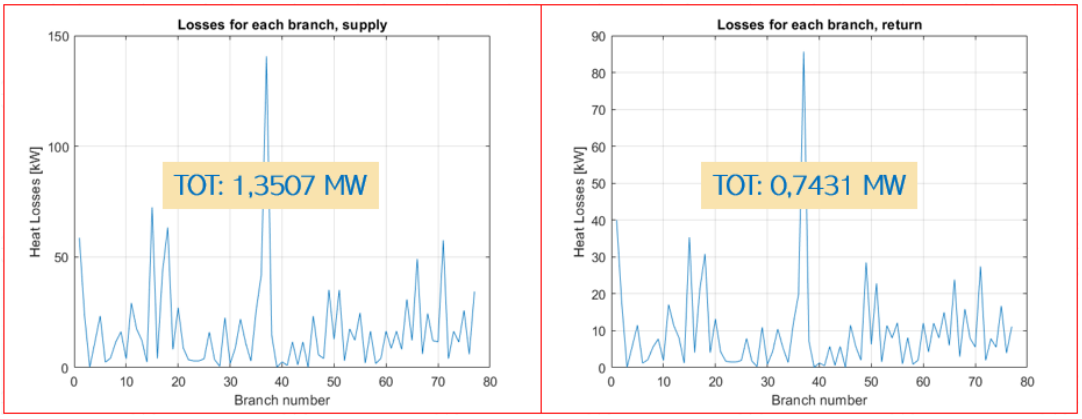

Figure 46: Heat losses of each branch at steady state for supply and return line

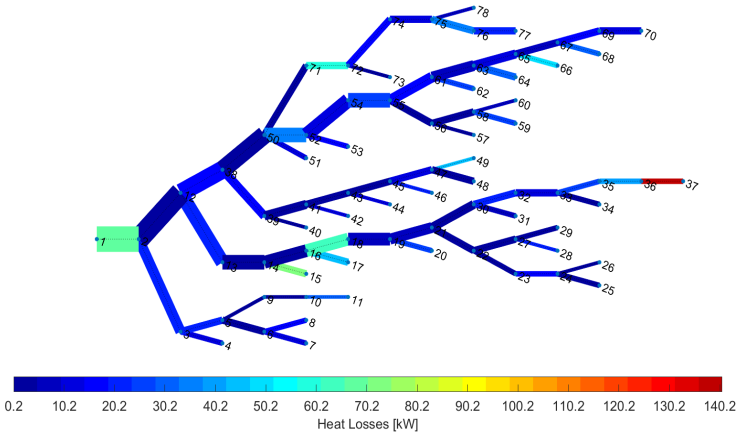

Figure 47: Heat losses for each branch

Also here the pattern does not have a relevant and significant order, it depends specially on the length of the branch.

Turning now to transient real model, the mass flow rate variation brings a pressure variation and a temperature variation during the day, according to the thermal

demand that users require. Two examples of industrial and non industrial node are provided. The profile of return line is equal but about $55°C$ lower.
The temperature profile follows the heat demand profile: for a higher thermal power required there is a higher mass flow rate, that means a lower thermal inertia so the hot water at $120°C$ is more easily transferred with less thermal losses, as already explained in figure 16.

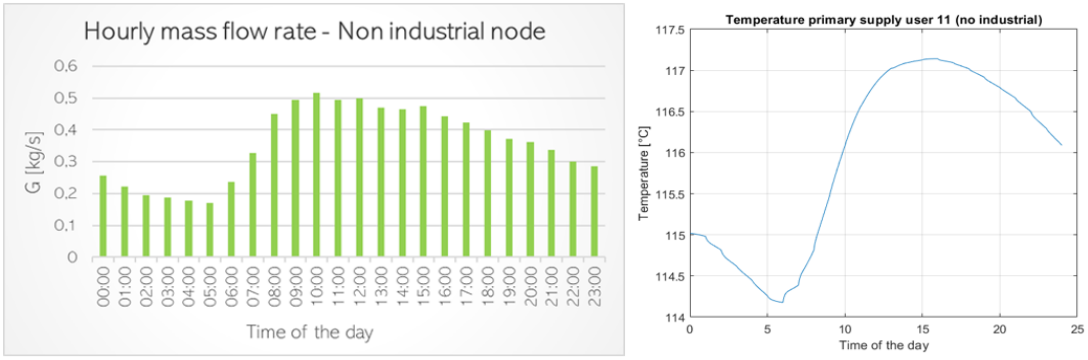

Figure 48: Mass flow rate and temperature in a day of January for a non industrial node

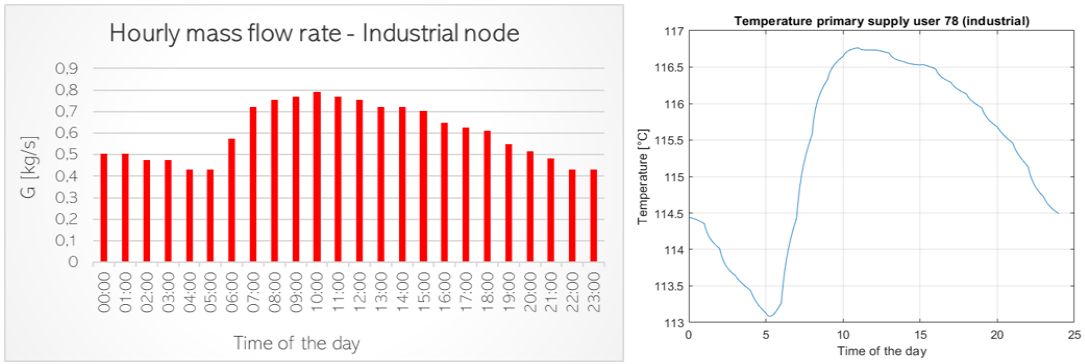

Figure 49: Mass flow rate and temperature in a day of January for an industrial node

As far as pressure losses are concerned, in a generic day of January they vary with the heat demand. The variation of mass flow rate strongly influences the pressure losses, that are quadratically proportional to the velocity. The pressure profile at maximum and minimum load is presented in figure 50.

The Δp_{max} in the total line is of 1.616 bar, but the difference with respect to the minimum mass flow rate configuration is remarkable: in this case the maximum pressure loss in the line is about 0.4 bar.

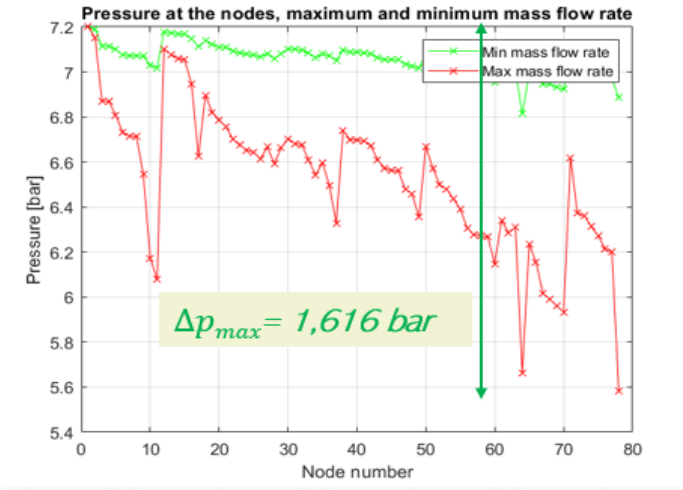

Figure 50: Maximum and minimum pressure profile in a day of January

In figure 51 is described the variation of pressure along the line: the values are obtained imposing a value of return in the plant of 2 bar, and a pressure drop at the user of 2 bar, too. So the total pumping system load can be calculated:

$$t_{PUMP} = 7.2 - 2 = 5.2\,bar \tag{58}$$

In figure 52 is represented the supply line with its pressures along the pipes, and here is highlighted the pressure drop at the user, the return pressure to the plant and the total pump load.

Now the analysis moves on one of the most important parameter of the study: the amount of thermal losses. During the day they follow the temperature profile, as can be imagined, and in the usual case of a generic January day shows up like in figure 53. This is because the ground temperature is supposed constant during the day, so the only parameter that changes during the day is the the network temperature. Thus the profiles are perfectly comparable. However the variations

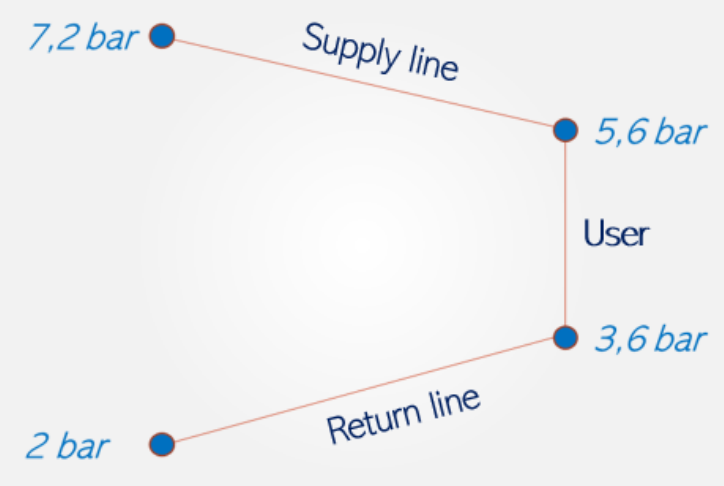

Figure 51: Pressure along the network

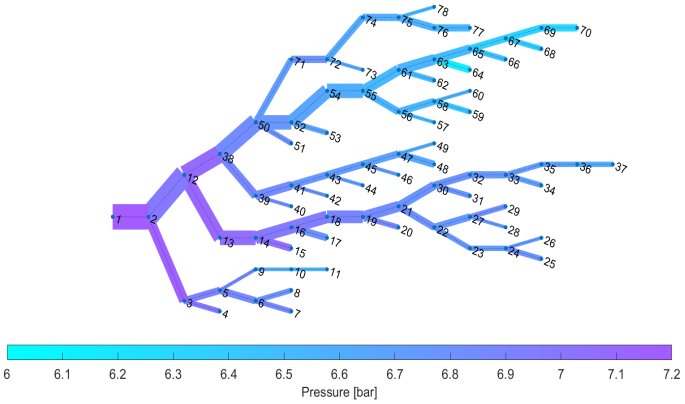

Figure 52: Pressure along the supply line

are limited.

Before turning to the annual analysis, the power profile and the percentage of losses with respect to thermal power are shown.

Finally also the residuals of SIMPLE algorithm are presented, in order to validate the results.

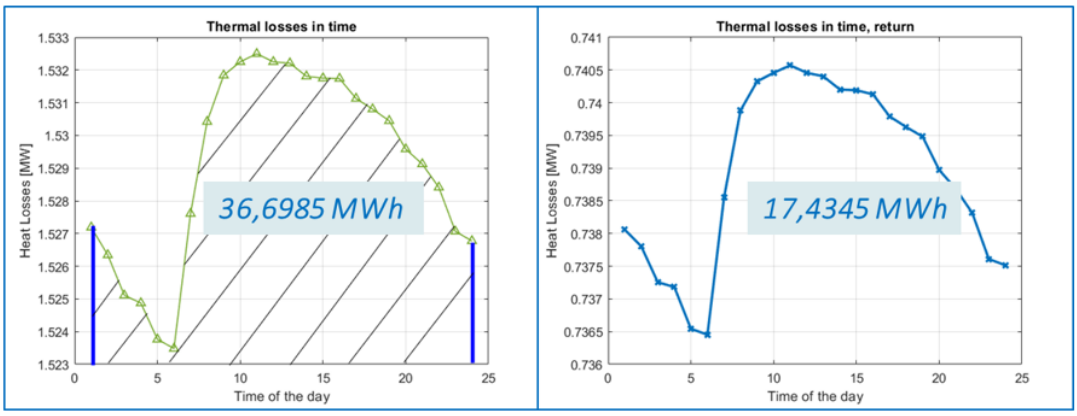

Figure 53: Daily profile of thermal losses

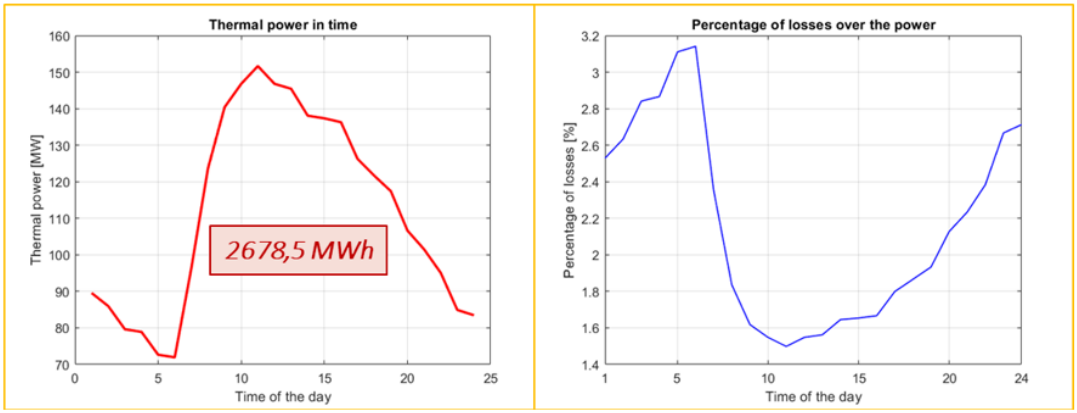

Figure 54: Daily profile of thermal power and percentage of losses

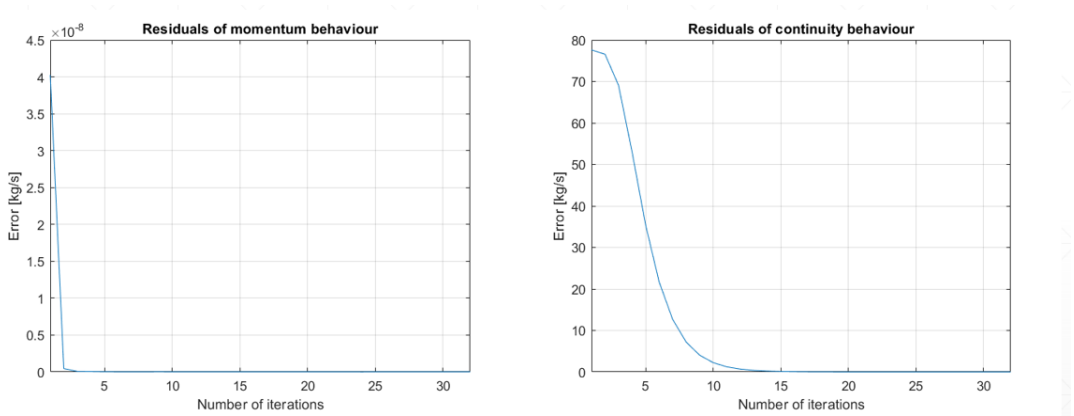

Figure 55: SIMPLE algorithm residuals

4.3.3 Annual results analysis

Once the daily behaviour of the system is described, it is necessary to analyze the system behaviour over an entire year, and then choose the best options for providing energy to the system studied.

The annual behaviour is studied by simulating every single day of the year with its own input data calculated in previous chapters. After that, all the data was collected and plotted in the following figures.

Figure 56: Pressure drop on supply line every day of the year

As already said, pressure drops are strongly dependent on mass flow rate. In summer the heat demand is very low, so it is mass flow rate and so are the pressure losses. From this the trend in figure 56.

In figure 57 is shown as the energy provided to the system in summer decreases a lot more than the thermal losses, because while the thermal request drops significantly, the temperature does not do the same, decreasing only of a few degrees.

This brings to the results shown in figure 58, that shows how the percentage, calculated on *energy*, varies from 2% in winter to 15% in summer, with an annual mean of 8.97%. The same percentage calculated instead om *power*, is about 2-3% because it is not affected by the high summer percentage weight.

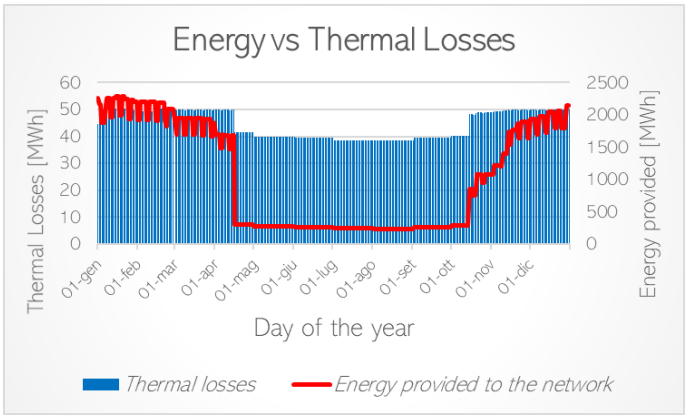

Figure 57: Energy provided to the system and total thermal losses along the year

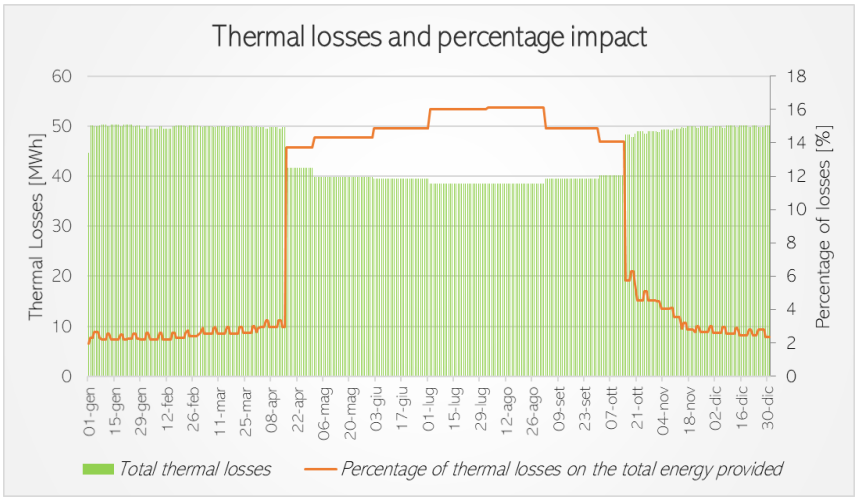

Figure 58: Total thermal losses along the year with correspondent percentage on the total energy provided

4.4 Production energy system design

At this time every detail of energy demand is known and calculated. For the purpose of this study two configurations of energy production are treated:

1. CASE 1: CENTRALIZED GENERATION

   In this case a single big plant, with an auxiliary boiler for peak demand is located in node 1. It is a centralized energy production configuration, in which all the thermal energy needed is produces in a single plant, and the hot water is heated up from the final return temperature to the supply temperature

($120°C$).

2. CASE 2: DISTRIBUTED GENERATION

   In this case the big plant power is reduced and supply temperature is decreased to $90°C$, trying to reduce thermal losses. This means that in order to reach the supply temperature at which the substations are designed to work there is the need of some thermal boosters that, near the users node, heats up the water to the requested temperature.

The choice of the type of energy production plants is the next step of the study. The possibilities for a district heating network with this kind of thermal demand are:

- Small (case 2) or medium (case 1) size cogeneration plants;
- WTE systems;
- Waste heat form industrial processes;
- Biomass boilers;
- Heat pumps (case 2);
- Solar collectors (in case 2).

The choice in this basic analysis is the first possibility of the four: it is the most used and the best one in order to analyze all the project also under an economic point of view. Moreover, the connection with electricity grid and gas network may open the doors for further and more detailed studies on energy networks.

4.4.1 Combined heat and power (CHP) technologies

The Combined Heat and Power energy production consists in the combined production of two different forms of energy with a single conversion process. Usually these forms of energy are electrical energy and thermal (heating or cooling) energy.

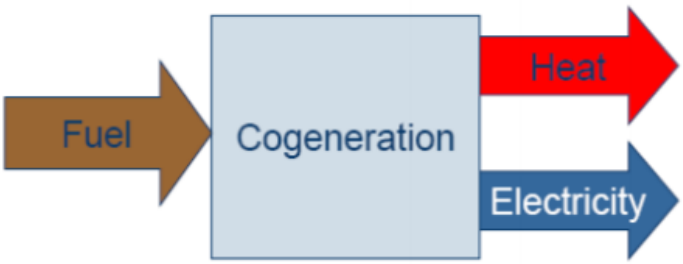

Figure 59: CHP production operating principle

The ratio between thermal and electrical energy produced is an important index in CHP production, and is strongly dependent on the technology used, as the table 8 of ARERA shows [22];

Table 8: Energy/Heat ratio for different CHP technologies

TECHNOLOGY	ENERGY/HEAT RATIO
Combined Cycle	0.95
Back pressure steam turbine	0.45
Condensation steam turbine	0.45
Gas turbine with heat recovery	0.55
Internal combustion engine	0.75

Some important parameters for cogeneration plants are the efficiencies:

$$\eta_{el} = \frac{E_{el}}{E_f} \tag{59}$$

$$\eta_{th} = \frac{E_{th}}{E_f} \tag{60}$$

$$\eta_{tot} = \frac{E_{el} + E_{th}}{E_f} \tag{61}$$

where E_{el} is the total amount of electrical energy produced, E_{th} the total thermal energy produced and E_f the primary energy consumption (fuel).
Another important index is the Primary Energy Saving, that identifies how much primary energy has been saved by producing energy in cogeneration configuration

instead of traditional one.

$$PES = 1 - \frac{1}{\frac{E_{th}}{\eta_{th,trad} \cdot E_c} + \frac{E_{el}}{\eta_{el,trad}}} \tag{62}$$

where η_{trad} is the efficiency of traditional energy production plants.

The most important advantages of cogeneration are the reduction of primary energy demand, due to the utilization of thermal energy that is usually dissipated in the environment and the lower electrical losses of transportation and distribution. Moreover this technology allows a reduction of environmental impact and a general saving for the purchase of energy.

The most relevant technologies for CHP production are:

- INTERNAL COMBUSTION ENGINES

  The advantages of this technologies are the big commercial availability (from some kW to 20 MW); the high electrical efficiency, until 45%; a good behaviour at partial loads, a high energy/heat ratio.

  But there are some fundamental problems for the use of this technology in this work. The first one is technical: these boosters have to heat up the water from $90°C$ to $120°C$, while the ICEs make available thermal heat until $95°C$, which is a too low value. The higher emissions and high maintenance cost exclude this technology from this study.

Figure 60: An internal combustion engine

These technology has one degree of freedom: available thermal power is univocally connected to electrical power. This means that a partial engine load,

both of energy fluxes decrease. This can be a problem in summer when the thermal energy needed by the district heating network is low, and it would be better to produce a high amount of electricity with a low heat production, in order to send more eletrical energy.

- GAS TURBINE

  Also this technology disposes of a high commercial availability, from micro-turbines of 30 kWe until big system of above 250 MWe. Moreover the GT are widely used and affordable, and the waste heat is at a high temperature ($500°C$). Also the costs are quite low.

  The drawbacks are the impossibility of intermittent operation and low electrical efficiency until medium size plants. In addition they have a low electricity/heat ratio.

  But for the purpose of this study they are the best option thanks to the modularity and the availability of high temperature heat.

Figure 61: A gas turbine

- OTHER TECHNOLOGIES

  An other important technology is steam turbine, but they are massive systems with extremely low electrical efficiency and energy/heat ratio.

  Other technologies under development are Fuel Cell and Heat Pumps, with an interesting future also under the point of view of environment protection.

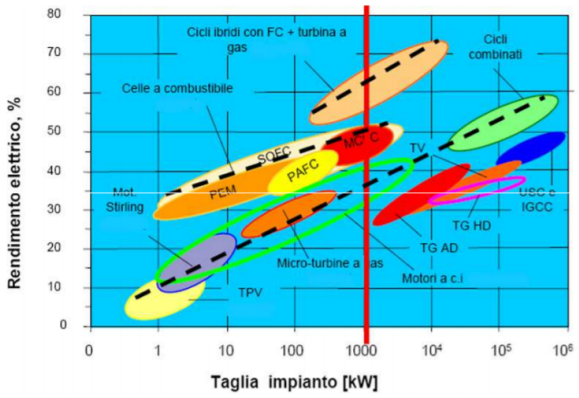

Figure 62: CHP technologies in function of available sizes and electrical efficiency [31]

4.4.2 Case 1: centralized generation

Thanks to the Matlab model it is possible to build the cumulative curve of thermal demand. The power calculated every hour is sorted in descending order and the figure 63 is obtained.

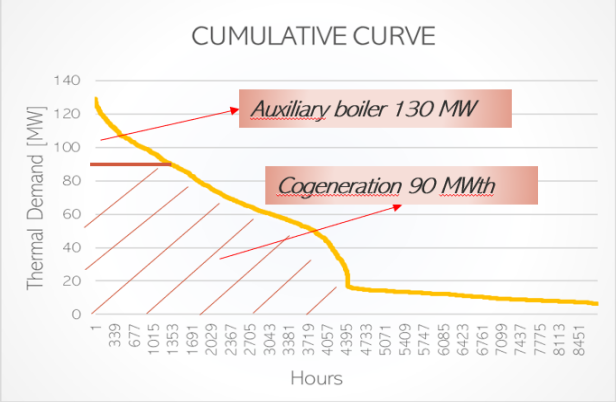

Figure 63: Cumulative curve of thermal demand

The best configuration in this case is a CHP plant based on a gas turbine of 90MWth and a coupling of electrical and thermal energy of this type: the cogeneration plant follows the user thermal profile, producing in each instant the energy power requested, and the electrical energy consequently produced is sold to the grid.

The configuration of the plant is described in figure 64.

		Annual thermal energy		Annual electrical energy		Power		Average annual efficiencies [%]	
GENERATION UNIT	*hours/year*	*[MWh]*	*[%]*	*[MWh]*	*[%]*	*P_el [MW]*	*P_th [MW]*	η_{el}	η_{th}
Gas Turbine	7435	241316	63,51	132724	100	50	90	0,35	0,6
Boiler	1325	138658	36,49	-	-	-	130	-	0,9

Figure 64: Configuration of the plant

4.4.3 Case 2: distributed generation

In this second case the hypothesis is to reduce the supply temperature of hot water from 120°C to 90°C in order to reduce thermal losses.

In order to make the comparison between the two cases sensible under a technological point of view, the supply temperature at the users must be maintained equal to the previous case. For this reason 21 thermal boosters have to be installed on the network, as figure 65 shows.

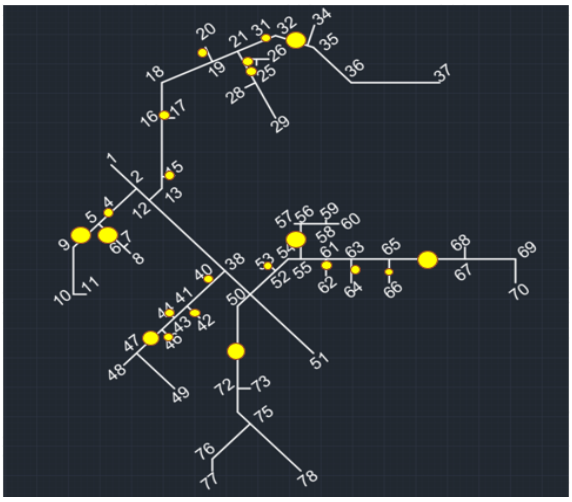

Figure 65: Yellow points identify the grid zones where the generated generation is installed

The temperature profile deriving from this modification of the system is the one presented in figure 66, while in figure 67 is presented in a more comprehensible scheme.

It can be seen how the nodes are at around 90°C until the thermal boosters intervene and heat up the water.

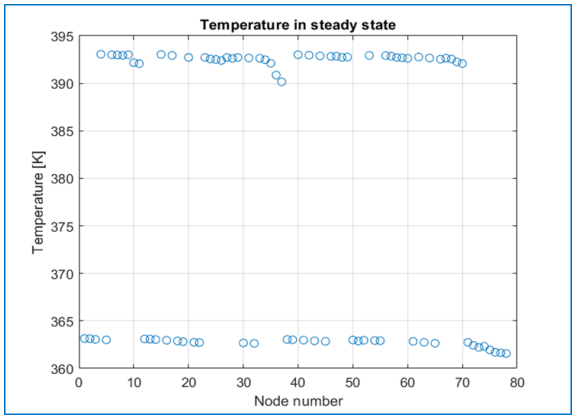

Figure 66: Temperature profile of supply line in case 2

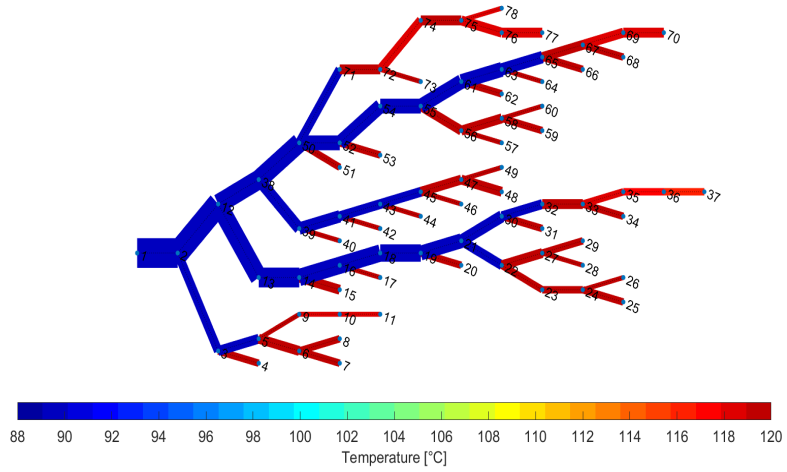

Figure 67: Temperature of supply line in case 2

Figure 68 shows, instead, how the thermal losses in configuration 2 are decreased of about 20% and the mean percentage on the total energy provided is down to 8.4% from the previous 9%.

With the same method of centralized distribution, the cumulative curves of these 21 boosters are calculated and presented in the following figures (example of node 1, the power plant, and an industrial and non industrial node.

This allows to half the thermal power of cogeneration plant, whose data are

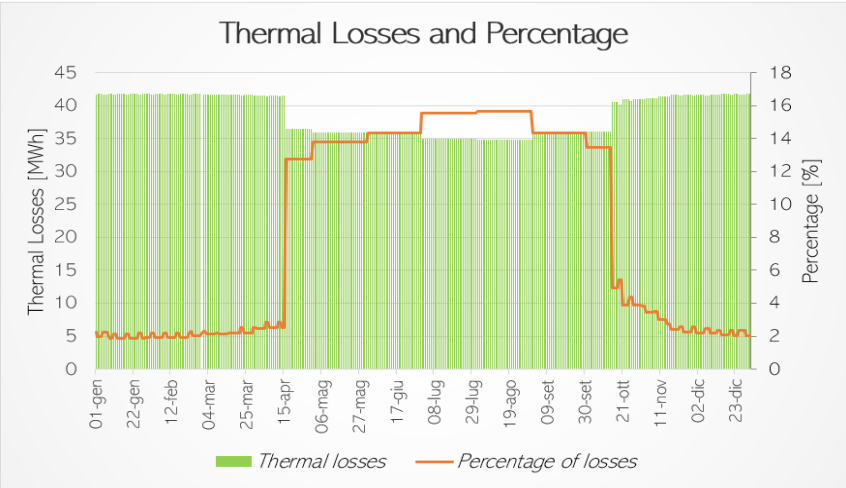

Figure 68: Total thermal losses along the year with correspondent percentage on the total energy provided

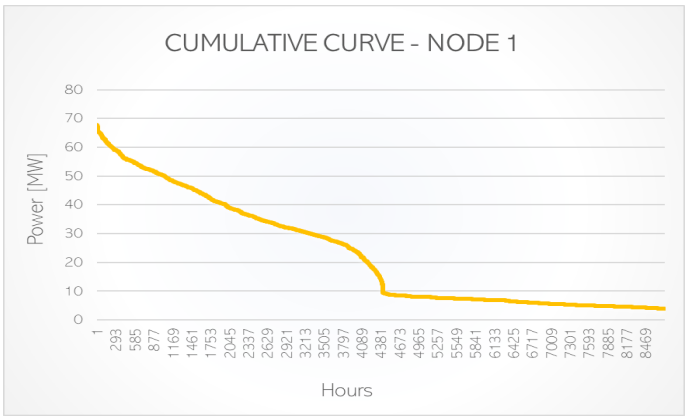

Figure 69: Cumulative curve of thermal demand for the plant

described in the table of fig 72.

In this case no auxiliary boiler are installed, because the small cogeneration plants are designed to follow the thermal load, and an extra heat production means also a higher electricity production, so higher incomes under an economic point of view. Moreover, it should be remember that this boosters are not boilers at the users, but they are located along the district heating network (supply line) in order to heat up the water in the desired points. So the cumulative curve has been obtained by multiplying the ΔT provided by the boosters by the mass flow rate that in that

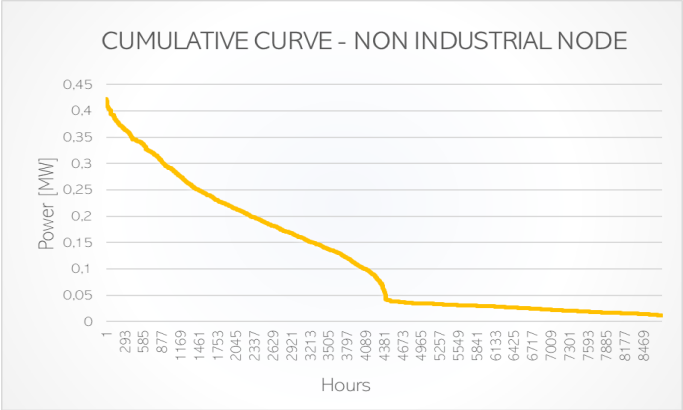

Figure 70: Cumulative curve of thermal demand for a non industrial user

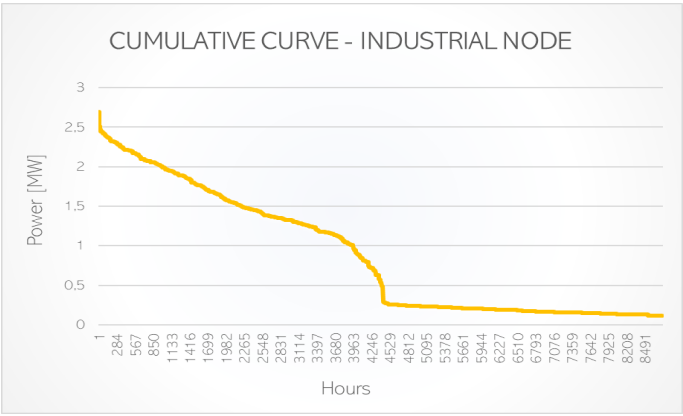

Figure 71: Cumulative curve of thermal demand for an industrial user

instant of time passes through that particular point.

		Annual thermal energy		Annual electrical energy		Power		Average annual efficiencies [%]		
GENERATION UNIT	*hours/year*	*[MWh]*	*[%]*	*[MWh]*	*[%]*	*P_el [MW]*	*P_th [MW]*	η_{el}	η_{th}	η_{tot}
Gas Turbine	7234	118766	32,02	65321	41,02	25	45	0,33	0,60	0,93
Boiler	1526	81427	21,95	-	-	-	68	-	0,9	-
Thermal Boosters	8760	170739	46,03	93907	58,98	0.23 - 2.9	0.4 - 5.3	0,32	0,58	0,90

Figure 72: Configuration of the plant

The thermal power of this boosters goes from 420 kW to 5.3 MW. For this reason they have been grouped in three different categories:

1. MICRO TURBINE

   This is the case of booster 11 and booster 14, that - considering the ratio

between electric power and thermal power equal to 0.55 - provide an electric power of, respectively, 250 KWe and 170 KWe.

Costruttore	Modello	Pe [kWe]	ηe [%]	ηt [%]	velocità [rpm]	β	T fumi [°C] (no CHP)
Capstone	**C30**	**30**	**26**	**-**	**96000**	**3.5**	**275**
Capstone	*C60*	*60*	*28*	*53.7*	*96000*	*3.7*	*360*
Capstone	**C65**	**65**	**29**	**50.0**	**96000**	**3.7**	**309**
Ingersoll Rand	*MT70*	*70*	*28*	*40.0*	*44000*	*-*	*210*
Bowman	**TG80CG**	**80**	**26**	**48.8**	**68000**	**-**	**278**
Elliott	*TA80*	*80*	*28*	*60.0*	*-*	*4.0*	*230*
Elliott	**TA100**	**100**	**29**	**50.0**	**-**	**4.0**	**293**
Turbec	**T100**	**100**	**30**	**46.5**	**70000**	**4.5**	**270**
Capstone	**C200**	**190**	**33**	**40.0**	**65000**	**-**	**280**
Ingersoll Rand	**MT250**	**250**	**30**	**44.6**	**45000**	**-**	**249**

Figure 73: Commercial micro-turbines

2. SMALL SIZE COGENERATION

   These are the plant with an electrical power lower than 1 MW and electrical efficiency of 0.32.

3. MEDIUM SIZE COGENERATION

   All the other plants, with an electrical efficiency of 0.33.

4.5 Primary energy and CO_2 emissions calculation

The first post-processing analysis is done in order to investigate energy improvements and consequently emissions savings. All the calculations are done for a year.

4.5.1 Case 0

The first step is the calculation of annual consumption of natural gas. This is possible thanks to the data of the table in figure 26, where it can be seen that the natural gas consumed in a year is $42,702,493\,Sm^3$.
From this value it is possible to calculate the primary energy demand in tonne of oil equivalent (toe). A toe corresponds to $4.187 \cdot 10^{10}\,[J]$.

Now it is necessary to calculate tonnes of oil equivalent to 1 Sm^3 of natural gas:

$$1\,[Sm^3] \cdot LHV\ \left[\frac{MJ}{Sm^3}\right] = 35.046\,MJ = 3.5046 \cdot 10^7\,[J] \tag{63}$$

This means that the conversion coefficient k_c from Sm^3 of natural gas to toe is:

$$k_c\left[\frac{Sm^3}{toe}\right] = \frac{4.187 \cdot 10^{10}}{3.5046 \cdot 10^7} = 1,195 \tag{64}$$

$$Q^0_{NG}\,[toe] = \frac{Q^0_{NG}\,[Sm^3]}{k_c} = 35,736.8\,toe \tag{65}$$

At this point the second parameter of the analysis must be studied. As explained in the introduction of this work one of the main aim of district heating network is to reduce Carbon Dioxide emissions in the atmosphere. In order to calculate the quantity of CO_2 that the combustion of natural gas releases in the atmosphere, the table in figure 9 is taken as reference. It is provided by the Italian Ministry of Environment (*MATTM, Ministero dell'ambiente e della tutela del territorio e del mare*).

Table 9: Emission factor from national inventory of UNFCCC (mean 2016-2018)

Combustibile	**U.d.m.**	**Fattore emissione (tCO_2/U.d.m.)**
Gas naturale (metano)	1000 $Stdm^3$	1.975

The emission factor that the Italian Ministry of Environment provides is

$$EF = 1.975\ \left[\frac{tCO_2}{1000\,Sm^3}\right] \tag{66}$$

This means that the tonnes of CO_2 emitted yearly from these users that burns natural gas for heating and hot water is:

$$Q^0_{CO2} = \frac{Q^0_{NG}\,[Sm^3]}{1000} \cdot EF = 42,702.493 \cdot 1.919 = 81,946.08\,ton_{CO2} \tag{67}$$

4.5.2 Case 1: substitution with centralized generation

In order to calculate the parameters that are object of this study the first thing to know is the natural gas consumption of this configuration. $E_{NG,plant}$ is the primary thermal energy provided with the combustion of natural gas in the plant, while $E_{NG,boiler}$ in the auxiliary boiler.

$$E_{NG,plant} = \frac{E_{el,plant}}{\eta_{el,plant}} = \frac{132,723}{0.35} = 379,211\,MWh \tag{68}$$

$$E_{NG,boiler} = \frac{E_{th,plant}}{\eta_{th,boiler}} = \frac{138,748}{0.9} = 154,164\,MWh \tag{69}$$

$$E_{NG,tot} = E_{NG,boiler} + E_{NG,plant} = 533,375\,MWh \tag{70}$$

Now with the Low Heating Value (LHV) of natural gas [25] it is possible to calculate the amount of fuel burned:

$$E_{NG,tot}\,[MJ] = E_{NG,tot}\,[MWh] \cdot 3600 = 1.920 \cdot 10^9\,MJ\ , \tag{71}$$

and consequently the primary energy consumption Q_{NG}.

$$Q^1_{NG} = \frac{E_{NG,tot}\,[MJ]}{LHV\ \left[\frac{MJ}{Sm^3}\right]} = 5.4789 \cdot 10^7\,[Sm^3] \tag{72}$$

With the conversion coefficient k_c the calculation of primary energy in *toe* is performed:

$$Q^1_{NG}\,[toe] = \frac{Q^1_{NG}\,[Sm^3]}{k_c} = 45,848.9\,toe\ , \tag{73}$$

and eventually the CO_2 emissions through the emission factor EF.

$$Q^1_{CO2} = \frac{Q^1_{NG}\,[Sm^3]}{1000} \cdot EF = 5.904 \cdot 10^4 \cdot 1.919 = 105,140.9\,ton_{CO2} \tag{74}$$

4.5.3 Case 2: substitution with distributed generation

The calculation of the previous parameters with input data of the case 2 configuration is here performed.

$E_{NG,plant}$ is the primary thermal energy provided with the combustion of natural gas in the plant, while $E_{NG,boiler}$ in the auxiliary boiler and $E_{NG,boost}$ in the total number of thermal boosters.

$$E_{NG,plant} = \frac{E_{el,plant}}{\eta_{el,plant}} = \frac{65,321}{0.33} = 197,944\, MWh \tag{75}$$

$$E_{NG,boiler} = \frac{E_{th,boiler}}{\eta_{th,boiler}} = \frac{81,427}{0.9} = 90,474\, MWh \tag{76}$$

$$E_{NG,boost} = \frac{E_{el,boost}}{\eta_{el,boost}} = \frac{93,907}{0.32} = 293,458\, MWh \tag{77}$$

$$E_{NG,tot} = E_{NG,boiler} + E_{NG,plant} + E_{NG,boost} = 581,876\, MWh \tag{78}$$

Now with the Low Heating Value (LHV) of natural gas [25] it is possible to calculate the amount of fuel burned:

$$E_{NG,tot}\,[MJ] = E_{NG,tot}\,[MWh] \cdot 3600 = 2.095 \cdot 10^9\, MJ\ , \tag{79}$$

and consequently the primary energy consumption Q_{NG}.

$$Q^2_{NG} = \frac{E_{NG,tot}\,[MJ]}{LHV\ \left[\frac{MJ}{Sm^3}\right]} = 5.977 \cdot 10^7\,[Sm^3] \tag{80}$$

With the conversion coefficient k_c the calculation of primary energy in *toe* is performed:

$$Q^2_{NG}\,[toe] = \frac{Q^2_{NG}\,[Sm^3]}{k_c} = 50,018\, toe\ , \tag{81}$$

and eventually the CO_2 emissions through the emission factor EF.

$$Q^2_{CO2} = \frac{Q^2_{NG}\,[Sm^3]}{1000} \cdot EF = 4.647 \cdot 10^4 \cdot 1.919 = 118,048.83\, ton_{CO2} \tag{82}$$

5 Economic Analysis

In order to analyze the economic feasibility [18] of this project in necessary to calculate OPEX and CAPEX of the entire installation:

- CAPEX is the initial investment cost that the plant owner pays at time t=0 (Total Plant Cost TPC).
- OPEX is the set of costs or incomes that every year, until the end of life of the plant, the plant itself produces.

Once this parameters are calculated, it is possible to implement a *cashflow analysis*. In this way all the movement of money can be identified: inflow (sale of goods and services, loans, lines of credit, asset sales) and outflow (business expenditures, loan payments, business purchases).
The *cashflow analysis* is performed from year 0 (the initial investment) until the end of life of the plant, that in this case is supposed to be 20 years. In the year 0 of construction is considered only the cost of investment. From year 1 on, instead, depreciation rate, incomes and operating cost (OPEX) have te be considered.
The *depreciation rate* DR is defined as:

$$DR = \frac{TPC\,[€]}{t_{dep}} \tag{83}$$

where TPC is the total plant cost and t_{dep} is the depreciation time, whose standard value is 10 years.

The parameters that has to be calculated in order to performed this analysis are:

- Total Plant Cost (TPC), which is practically the investment cost, so the total outflow of year 0 of construction:

$$CAPEX_{tot} = C_{inv,plant} + C_{inv,boilers} + C_{inv,pump} + C_{inst,network} \tag{84}$$

where C_{plant} is the total cost of investment needed to build the cogeneration plant and, in the second case, all the thermal boosters; $C_{boilers}$ is the cost of construction of auxiliary boilers, C_{pump} cost of construction of pumping system and $C_{network}$ is the cost of installation of district heating network in the urban area.

- The overall yearly cost for the following years (from 1 to 20), defined as:

$$Costs\left[\frac{€}{year}\right] = C_{OPEX,plant} + C_{OPEX,boilers} + C_{OPEX,pump} + C_{maint,network} \quad (85)$$

where all the OPEX cost are yearly maintenance costs for those systems.

- The Incomes, which are calculated depending on the subsidy for energy exported to the grid:

$$Incomes\left[\frac{€}{year}\right] = Incomes_{el} + Incomes_{th} \quad (86)$$

where $Incomes_{el}$ come from the electrical energy sold and $Incomes_{th}$ from the thermal energy sold.

Once all these parameters are known, the cash flow can be eventually calculated:

$$Cash\,flow\left[\frac{€}{year}\right] = Incomes - Costs - t \cdot (Incomes - Costs - DR) \quad (87)$$

where t is the tax rate (in Italy is considered $t = 0.43$) which has to be applied only if $Incomes - Costs > 0$; while DR (Depreciation Rate) has to be applied only for the depreciation time, i.e. for the first 10 years.

At this point a method is necessary in order to consider the present value of money, in this way the present cash flow and the Net Present Value (NPV), Pay

Back Time (PBT) can be analyzed.

$$Present\,cash\,flow\left[\frac{€}{year}\right] = Cash\,flow\,\cdot\,Discounting\,factor \tag{88}$$

where Discounting factor is defined as

$$Discounting\,factor = (1 + WACC)^{-(n-n_0)} \tag{89}$$

WACC is Weight Average Cost of Capital, and it takes into account which percentage of the initial investment is covered by debt and which by equity. It is expressed as:

$$WACC = k_e \cdot c_e + k_d \cdot c_d \cdot (1 - t) \tag{90}$$

where k_d is the percentage of debt, k_e the percentage of equity, c_d the cost of debt, c_e the cost of equity.

At this point the Cumulative Cash Flow (CCF) can be determined as

$$CCF_j = \sum_{n=0}^{j} Present\,cash\,flow_n \tag{91}$$

The year in which the CCF stars to be positive ($Net\,Present\,Value > 0$) is the year in which all the project starts to earn money, and it is called *Payback Time*, PBT.

5.1 Case 1: Centralized generation

5.1.1 CAPEX

1. COGENERATION PLANT

   In order to estimate the quantities defined in the previous chapter, the values in figure 74 [19],[20] have been considered.

   In this case the $C_{inv,plant}$ is simple to calculate, knowing the unit cost $c_{inv,plant}$

Global efficiency [%]	35
Investment cost [k€/MW]	900
Yearly O&M costs [k€/MW-year]	40
Fuel cost [€/Gcal]	33,8
Lifetime [year]	20
Capacity factor	0,85

Figure 74: Parameters taken into consideration for economic analysis

in table 74:

$$C_{inv,plant} = c_{inv,plant} \left[\frac{€}{MW}\right] \cdot P_{el,plant}\,[MWe] = 900,000 \cdot 50 = 45,000,000 €$$ (92)

2. AUXILIARY BOILER

The italian GSE (Gestore Servizi Energetici) provides the following table (75) that summarizes the costs for a boiler.

	C_{inv}	$C_{o\&m}$	$C_{o\&m}$	C_{fuel}	R_{heat}	$R_{ele\ chp}$ invernale	R_{ele} solo ele estivo
	€/KW	€/KWanno	€/MWh	€/KWh	€/MWh	€/MWh	€/MWh
MCI grande taglia	650	52		0,027	94,8	57	78
MCI piccola taglia	1000	40		0,027	94,8	57	78
Caldaia a gas	100		3	0,028	94,8	57	78

Figure 75: Economic costs provided by GSE [17]

These data are taken from a GSE study [17] that concerns the application of CHP production with district heating. The value of R are calculated taking into consideration industrial investment, operating and financial costs. It strongly depend also on retail to the users price.

Following these data the investment cost for auxiliary boiler is easily calculated as:

$$C_{inv,boiler} = c_{inv,boiler} \left[\frac{€}{MW}\right] \cdot P_{el,boiler}\,[MWe] = 100,000 \cdot 130 = 13,000,000 €$$ (93)

3. DISTRICT HEATING NETWORK INSTALLATION

In order to calculate CAPEX of distribution network it is necessary to know the unit cost per meter of pipe, depending on pipe diameter, as explained in figure 76.

D [mm]	*€/m*
25	114
50	145
100	415
150	517
200	620
250	700
300	775
350	930
400	954
450	994
500	1017
600	1020

Figure 76: Unit installation cost for distribution network [16] [15]

In the case of the network taken into consideration these data evolve in the following costs:

Total length [m]	*D [mm]*	*Installation cost [€]*
283	600	288660
141	500	143397
1373	400	1309842
1238	350	1151340
1143	300	885825
685	250	479500
5527	200	3426740
2525	150	1305425
2251	100	934165
TOTAL COST		*9924894*

Figure 77: Total installation cost for distribution network

An other point of CAPEX is the installation of substations in order to link the network to the users, that can be approximated as 30% of investment cost [17]:

$$C_{substation} = 0.3 \cdot 9,924,894 = 2,977,468\,€ \tag{94}$$

Once obtained these values $C_{inst,network}$ can be calculated as:

$$C_{inst,network} = C_{inst,pipe} + C_{substation} = 12,902,362 € \tag{95}$$

4. PUMPING SYSTEM

   The investment cost of the pumping system is considered as 450,000€ for a 400 kW system [21].

So the total investment cost at year 0 of construction, according to equation (84), is:

$$CAPEX_{tot} = 32,400,000 + 13,000,000 + 12,902,362 + 450,000 = 58,752,362 € \tag{96}$$

5.1.2 OPEX

1. COGENERATION PLANT

   Always following figure 74, the yearly unit cost linked to Operation & Maintenance ($c_{O\&M,plant}$) is equal to 40,000$/MW that, considering the current exchange rate (0.91, [24]), becomes:

$$c_{O\&M,plant}[€] = c_{O\&M,plant}[\$] \cdot 0.91 = 36,400 € \tag{97}$$

$$C_{O\&M,plant} = C_{inv,plant} \cdot P_{el,plant} = 36,400 \left[\frac{€}{MW}\right] \cdot 50\,[MW] = 1,820,000\,\frac{€}{year} \tag{98}$$

   The other operational cost is the energy source: natural gas. In order to estimate this cost, with reference to ARERA [22], the price of natural gas is estimated being 29 €/MWh. These MWh is the quantity of energy produced burning the natural gas and it is obtained by dividing the quantity of electrical

energy produced in a year by the thermal efficiency:

$$E_{NG} = \frac{E_{el}}{\eta_{el}} = \frac{132,724}{0.35} = 379,211\,MWh \tag{99}$$

The operation in equation 99 is possible because the value of LHV provided by this authority (the same ARERA) it is the value that has been used in this work. At this point it is possible to estimate the annual cost of natural gas of the cogeneration plant:

$$C_{NG,plant} = E_{NG} \cdot c_{NG} = 10,617,912\,\frac{€}{year} \tag{100}$$

At the end it can be calculated the total operational plant cost:

$$C_{OPEX,plant} = C_{O\&M,plant} + C_{NG,plant} = 12,437,912\,\frac{€}{year} \tag{101}$$

2. AUXILIARY BOILER

   Looking at figure 75, the unit cost of operation & maintenance for boilers is 3 €/MWh, consequently:

$$C_{O\&M,boiler} = c_{O\&M,boiler} \cdot E_{boiler}[MWh] = 3 \cdot 138,748 = 416,245\,\frac{€}{year} \tag{102}$$

   Also in the case of auxiliary boiler the natural gas cost has to be considered:

$$C_{NG,boiler} = c_{NG,boiler} \cdot \frac{E_{boiler}}{\eta_{boiler}} = 29 \cdot \frac{138,748}{0.9} = 4,313,813\,\frac{€}{year} \tag{103}$$

   and the total operational cost is:

$$C_{OPEX,boiler} = C_{O\&M,boiler} + C_{NG,boiler} = 4,730,057\,\frac{€}{year} \tag{104}$$

3. DISTRICT HEATING NETWORK

Concerning the OPEX, the network unit maintenance $c_{maint,network}$ can be identified in the value of 1.9 €/MWh [17], that multiplied for the total energy provided to the network (E_{TOT}) can bring to the total OPEX cost of the network.

$$C_{OPEX,net} = c_{O\&M,net} \cdot E_{tot} = 1.9 \cdot 379,974.426 = 721,951 \frac{€}{year} \tag{105}$$

4. PUMPING SYSTEM

   The operating cost for pumping system ($c_{OPEX,pump}$) can be approximated as 1.6 €/MWh [15]. The yearly energy provided by the pumps to the network E_{pump} has already been calculated and it is equal to 1266 MWh, but that unit cost refers to the heat provided to the system, thus:

$$C_{OPEX,pumps} = c_{OPEX,pumps} \cdot E_{TOT} = 386,106 \frac{€}{year} \tag{106}$$

Now that all the costs are calculated it necessary to evaluate the Incomes described in previous chapter. As already explained the Incomes are composed of two different terms, because the owner of the cogeneration plant sells both electricity to grid and thermal energy to the district heating network users.
The unit revenue for the sale of electrical energy and heat for district heating can be observed in figure 75: $r_{sale,el} = 57 €/MWh$ (78 in summer) and $r_{sale,th} = 94.8 €/MWh$. In this way the incomes can be calculated:

$$Incomes_{el} = r_{sale,el} \cdot E_{el} = 8,262,062 \frac{€}{year} \tag{107}$$

$$Incomes_{th} = r_{sale,th} \cdot (E_{TOT} - E_{loss}) = 34,477,986 \frac{€}{year} \tag{108}$$

5.1.3 Cashflow Analysis

First point of the analysis is the depreciation rate DR, calculated as:

$$DR = \frac{CAPEX_{tot}}{t_{dep}} = \frac{71,352,362}{10} = 7,135,236.2 €$$ (109)

Consequently, the DR has to be applied only for the first 10 years. This brings to two different definitions of $Cash\,Flow$:

$$Cash\,Flow_1 \left[\frac{€}{year}\right] = Incomes - Costs - t \cdot (Incomes - Costs - DR)$$ (110)

for the first 10 years and

$$Cash\,Flow_2 \left[\frac{€}{year}\right] = Incomes - Costs - t \cdot (Incomes - Costs)$$ (111)

for the remaining years.
Weighted Average Cost of Capital for calculation of discounting factor is estimated to be 5% [17]. With these data it is possible to calculate all the parameters required, as the figure 78 shows.

For the calculation of the Payback Time a linear approximation of NPV curve is applied from year 4 to 5. In this way a line is constructed and imposing the CCF equal to 0 it is possible to find the point in which the NPV curve meets the x-axis:

$$PBT = 4 + \frac{11,026,368}{2,303,484 + 11,026,368} = 4.83\,years$$ (112)

This means that after less than 5 years all the money spent in the initial investment is recovered.

The Net Present value at 20 years that is equal to NPV=126,118,292 €.

ANNO	Cash flow	DISCOUNTING FACTOR	Present Cash Flow	Cumulative Cash Flow
0	-71352362	1,00	-71352362	-71352362
1	17012644	0,95	16202518	-55149844
2	17012644	0,91	15430970	-39718874
3	17012644	0,86	14696162	-25022712
4	17012644	0,82	13996345	-11026368
5	17012644	0,78	13329852	2303484
6	17012644	0,75	12695097	14998581
7	17012644	0,71	12090569	27089150
8	17012644	0,68	11514827	38603977
9	17012644	0,64	10966502	49570479
10	17012644	0,61	10444288	60014767
11	13944493	0,58	8153056	68167823
12	13944493	0,56	7764815	75932639
13	13944493	0,53	7395062	83327701
14	13944493	0,51	7042916	90370617
15	13944493	0,48	6707539	97078157
16	13944493	0,46	6388133	103466289
17	13944493	0,44	6083936	109550225
18	13944493	0,42	5794225	115344450
19	13944493	0,40	5518309	120862759
20	13944493	0,38	5255533	126118292

Figure 78: Cash flow analysis (case 1)

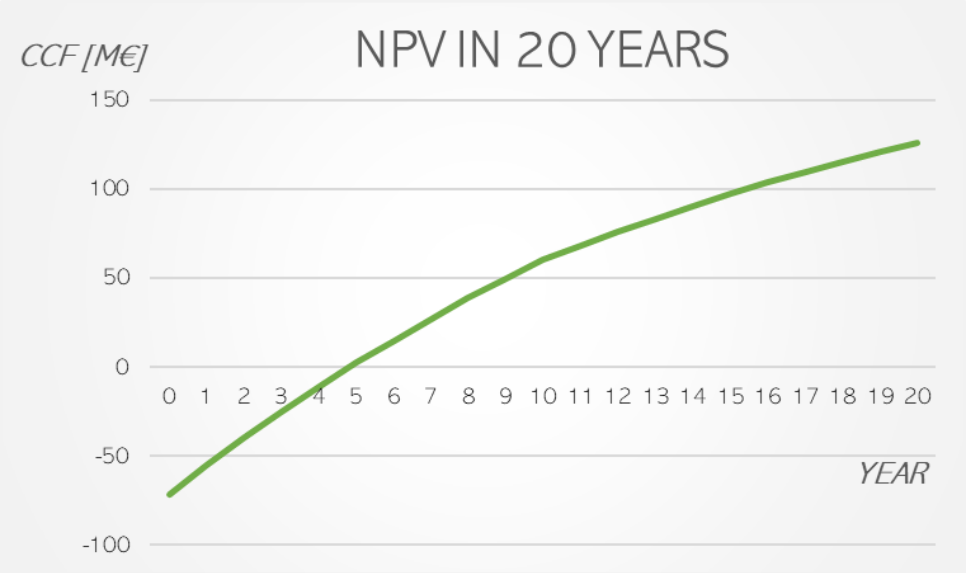

Figure 79: Cumulative Cash Flow for every year of system lifetime (case 1)

5.2 Case 2: Distributed Generation

1. COGENERATION PLANT

   The procedure is similar to the plant of case 1, with different values, like figure 80 shows [19],[20].

Electrical efficiency [%]	32
Investment cost [k€/MW]	1000
Yearly O&M costs [k€/MW-year]	45
Fuel cost [€/Gcal]	33,8
Lifetime [year]	20
Capacity factor	0,83

Figure 80: Parameters taken into consideration for economic analysis

In this case the $C_{inv,plant}$ is:

$$C_{inv,plant} = c_{inv,plant} \left[\frac{€}{MW}\right] \cdot P_{el,plant}\,[MWe] = 1,000,000 \cdot 25 = 25,000,000\,€ \tag{113}$$

Always following figure 74, the yearly unit cost linked to Operation & Maintenance ($c_{O\&M,plant}$) is equal to 45,500€/MW:

$$C_{O\&M,plant} = c_{O\&M,plant} \cdot P_{el,plant} = 45,500 \left[\frac{€}{MW}\right] \cdot 25\,[MW] = 1,137,500\,\frac{€}{year} \tag{114}$$

Always with reference to ARERA [22], the price of natural gas is estimated being 29 €/MWh.

$$E_{NG} = \frac{E_{el}}{\eta_{el}} = \frac{65,321}{0.33} = 197,943.8\,MWh \tag{115}$$

At this point it is possible to estimate the annual cost of natural gas of the cogeneration plant:

$$C_{NG,plant} = E_{NG} \cdot c_{NG} = 5,740,330\,\frac{€}{year} \tag{116}$$

At the end it can be calculated the total operational plant cost:

$$C_{OPEX,plant} = C_{O\&M,plant} + C_{NG,plant} = 6,877,830 \frac{€}{year} \tag{117}$$

2. AUXILIARY BOILER

Figure (75) is valid also for this case, so the calculation can proceed:

$$C_{inv,boiler} = c_{inv,boiler} \left[\frac{€}{MW}\right] \cdot P_{el,boiler}\,[MWe] = 100,000 \cdot 68 = 6,800,000 € \tag{118}$$

Looking at figure 75, the unit cost of operation & maintenance for boilers is 3 €/MWh, consequently:

$$C_{O\&M,boiler} = c_{O\&M,boiler} \cdot E_{boiler}[MWh] = 3 \cdot 81,427 = 244,281 \frac{€}{year} \tag{119}$$

Also in the case of auxiliary boiler the natural gas cost has to be considered:

$$C_{NG,boiler} = c_{NG,boiler} \cdot \frac{E_{boiler}}{\eta_{boiler}} = 29 \cdot \frac{81,427}{0.9} = 2,623,759 \frac{€}{year} \tag{120}$$

and the total operational cost is:

$$C_{OPEX,boiler} = C_{O\&M,boiler} + C_{NG,boiler} = 2,868,040 \frac{€}{year} \tag{121}$$

3. THERMAL BOOSTERS

For the evaluations of the costs of micro-turbine, mini and medium size cogeneration cost curves have been applied in order to consider the different size of each booster. The data for the construction of these curves ([23]) have been gathered and sorted plots in figure 81 and 82:

It is possible to notice that these costs are higher than the unit cost of case 1, this because in the case of smaller sizes the amount of money that is necessary

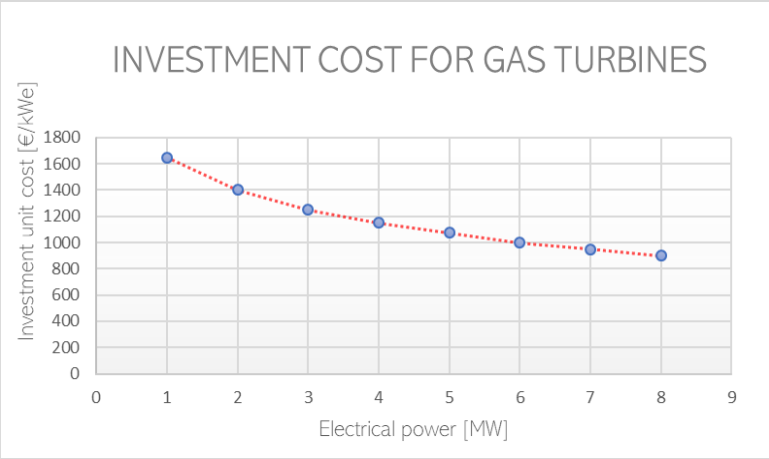

Figure 81: Unit investment cost for the construction of gas turbines [23]

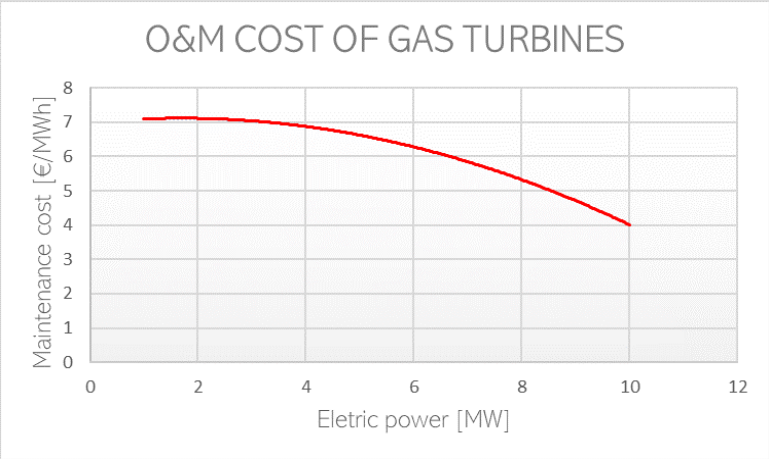

Figure 82: Unit Operation & Maintenance cost for gas turbines [23]

to spend for a single unit of energy increases.

Due to the different configuration (at lower temperature) the energy that the system has to provide to district heating network is slightly reduced, thanks to the lower thermal losses. Nevertheless this little drop of thermal demand is not sufficient to justify the higher investment that distributed generation requires, as will be clarified below.

Knowing these data the calculation of the total costs of the thermal boosters

is performed.

$$C_{inv,boost} = c_{inv,boost} \left[\frac{€}{MW}\right] \cdot \sum_j P_j^{el,boost} [MWe] = 31,176,092 € \tag{122}$$

$$C_{O\&M,boost} = c_{O\&M,boost} \cdot \sum_j E_{boost}[MWh] = 1,878,986 \frac{€}{year} \tag{123}$$

Also in the case of thermal boosters the natural gas cost has to be considered:

$$C_{NG,boost} = c_{NG} \cdot \frac{E_{el,boost}}{\eta_{el,boost}} = 29 \cdot \frac{93,906.6}{0.32} = 8,510,286 \frac{€}{year} \tag{124}$$

and the total operational cost is:

$$C_{OPEX,boost} = C_{O\&M,boost} + C_{NG,boost} = 10,389,272 \frac{€}{year} \tag{125}$$

4. OTHER POINTS

   District heating network and pumping system are supposed not to vary with respect to case 1.

The unit revenue for the sale of electrical energy and heat for district heating are the same of previous case: $r_{sale,el} = 57 €/MWh$ (78 in summer) and $r_{sale,th} = 94.8 €/MWh$. In this way the incomes can be calculated:

$$Incomes_{el} = r_{sale,el} \cdot E_{el} = 9,911,947 \frac{€}{year} \tag{126}$$

$$Incomes_{th} = r_{sale,th} \cdot (E_{TOT} - E_{loss}) = 33,829,907 \frac{€}{year} \tag{127}$$

Supposing other parameters for cash flow analysis unchanged it is possible to perform the calculation done for case 1 with the new input data, obtaining the following.

The calculation of the Payback Time is performed with the same method of the

ANNO	Cash flow	DISCOUNTING FACTOR	Present Cash Flow	Cumulative Cash Flow
0	-76328454	1,00	-76328454	-76328454
1	16412805	0,95	15631243	-60697212
2	16412805	0,91	14886898	-45810314
3	16412805	0,86	14177998	-31632316
4	16412805	0,82	13502855	-18129461
5	16412805	0,78	12859862	-5269599
6	16412805	0,75	12247488	6977889
7	16412805	0,71	11664274	18642163
8	16412805	0,68	11108832	29750995
9	16412805	0,64	10579840	40330835
10	16412805	0,61	10076038	50406874
11	13130681	0,58	7677237	58084111
12	13130681	0,56	7311655	65395766
13	13130681	0,53	6963481	72359246
14	13130681	0,51	6631886	78991133
15	13130681	0,48	6316082	85307215
16	13130681	0,46	6015316	91322531
17	13130681	0,44	5728873	97051404
18	13130681	0,42	5456069	102507473
19	13130681	0,40	5196256	107703730
20	13130681	0,38	4948816	112652545

Figure 83: Cash flow analysis for case of distributed generation

previous case:

$$PBT = 5 + \frac{5,269,599}{6,977,889 + 5,269,599} = 5.43\, years \tag{128}$$

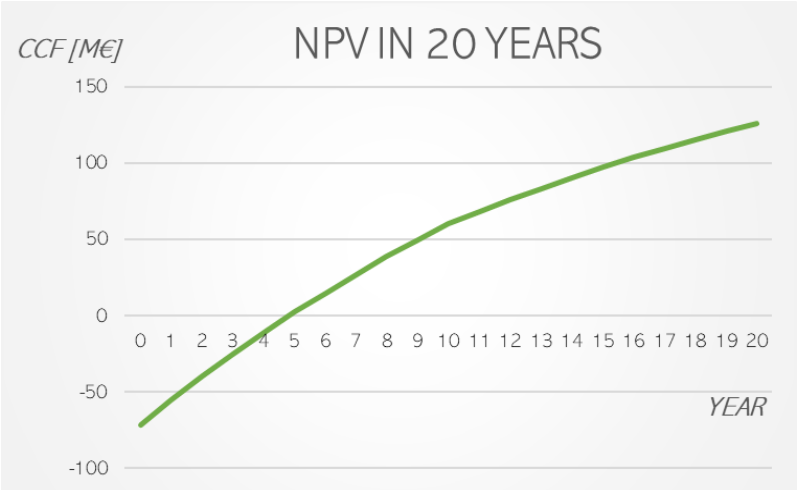

Figure 84: Cumulative Cash Flow in time for distributed generation case

The Net Present value at 20 years that is equal to NPV=112,652,545 €.

6 Comparison between the configurations

In this chapter a global analysis of the critical aspects of the three different configurations is proposed. With different criteria, the cases are compared in order to establish the best one.
After all the simulation done the post-processing allows to extract all the values useful for this analysis.

6.1 Energy saving and CO2 emissions

The first comparison is done under the primary energy point of view. In chapter 4.5 was performed the calculation of primary energy for the three case, here summarized in figure 85.

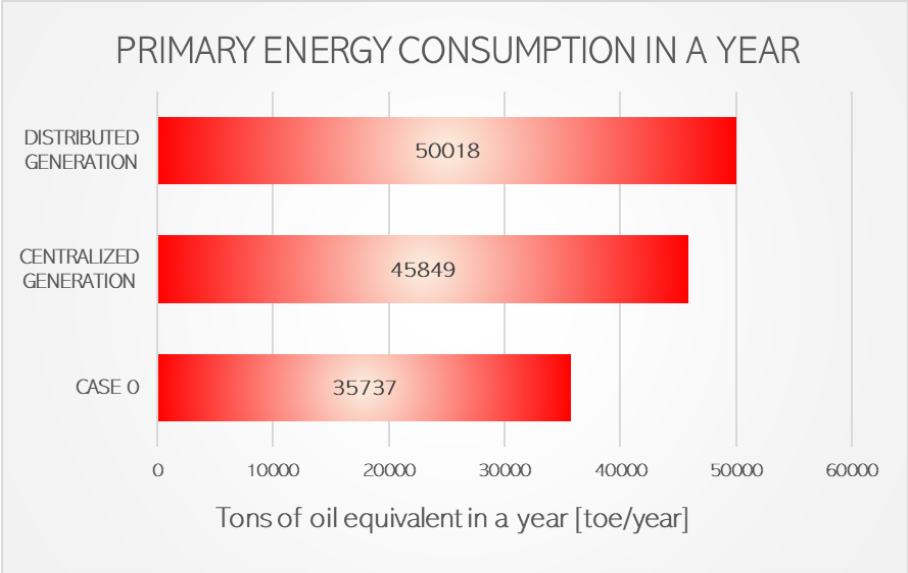

Figure 85: Primary energy consumption of the three configurations

As it can be noticed from the plot, from the case 0 (lowest consumption) to the case 2 (highest consumption) there is a difference of almost 30%. The reasons for that are two:

- The cogeneration plants: these are plants that have a lower thermal efficiency

with respect to the local small size boilers. On the other hand they have also an electrical efficiency because they produce both electricity and heat: this is an aspect that has to be taken into consideration for a complete and coherent analysis.

- The smaller size of plants in case 2: in the distributed heat generation case the size of the thermal boosters is obviously smaller than the case of a big plant. This implies a smaller efficiency of the single booster with respect to the higher size plant.

Always in chapter 4.5 the procedure for the calculation of CO_2 emissions is described, and the values obtained are listed. Here are represented in the plot of figure 86.

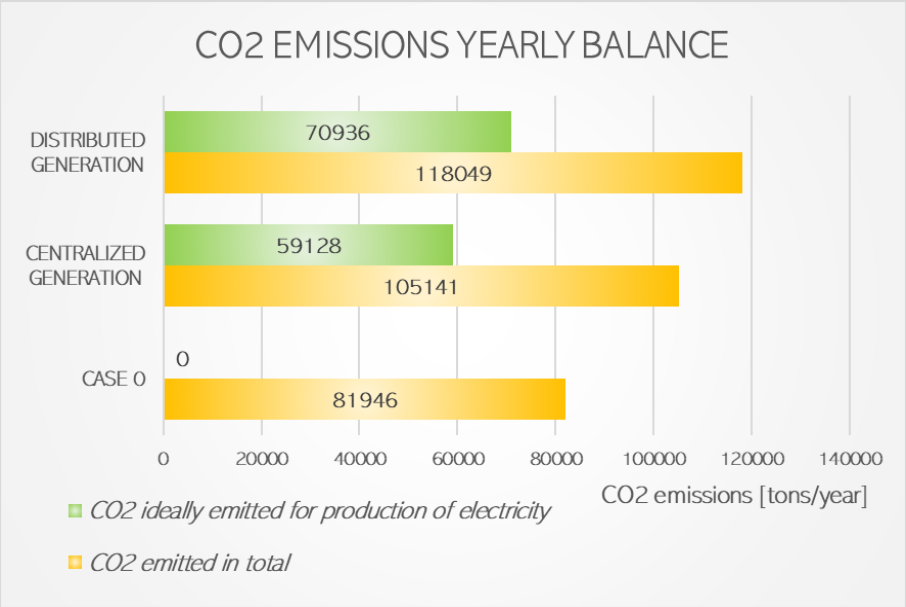

Figure 86: CO_2 emissions for the three configurations

The orange bars represent the CO_2 emitted in a year in total while the green bar represents the Carbon Dioxide that would have been emitted in order to produce the electrical energy produced in the plants. In order to perform this calculation the medium global efficiency for the production of electrical energy is considered equal

to 41,50%, as given by ISPRA Ambiente website [26].

For the sake of clarification the green bars identify *fictitious* emissions: it would be emitted if the electrical energy produced in the cogeneration plants was produced by a generic plant in Italy.

This means that for the total balance aimed at evaluate the best project, the quantity of CO_2 ideally emitted for electricity production must be subtracted from the total emissions, in order to compare the three cases only regarding to the heating purposes. This process has been done in figure 87.

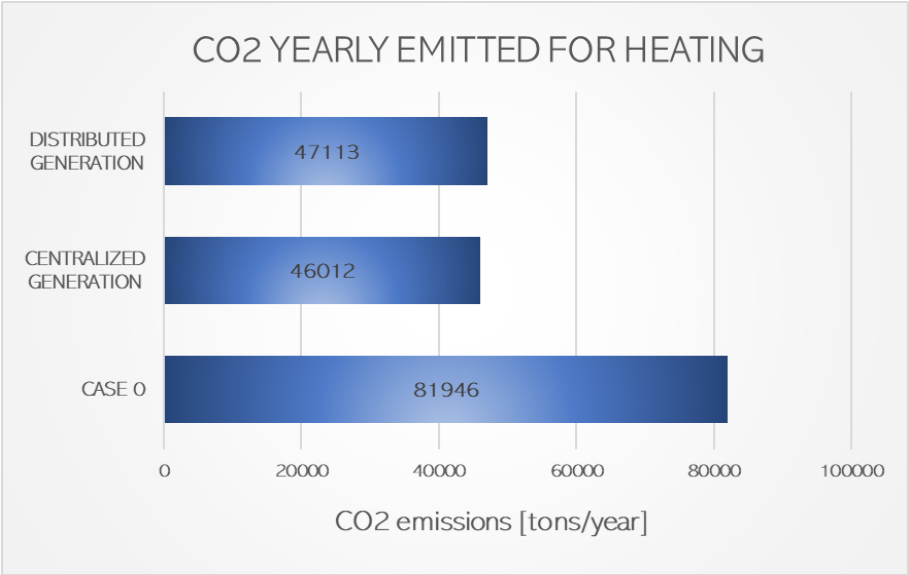

Figure 87: CO_2 emitted for heating purpose

Here the situation is changed. Until now data seem to suggest that the best case among the three was the first, with a lower primary energy consumption and consequently lower emissions. The two first plots were nonetheless only partially accurate: the three configurations compared have different scopes. Case 1 and 2 contain plants designed for cogeneration purposes, that change the cards of evaluation. Proper indices are needed in order to coherently analyze the systems, an one is the Carbon Dioxide emissions only considering space and water heating purposes. As it can be seen in the plots these emissions are halved in case of district heat-

ing network with respect to the case without it, and in particular the centralized generation is even better than the distributed generation. The main reason is that, despite a higher production of electricity in case 2, the efficiencies of small plants are lower than the efficiency of a single big plant. An other index useful in order to properly compare the cases is the useful energy for unit of primary energy (figure 88).

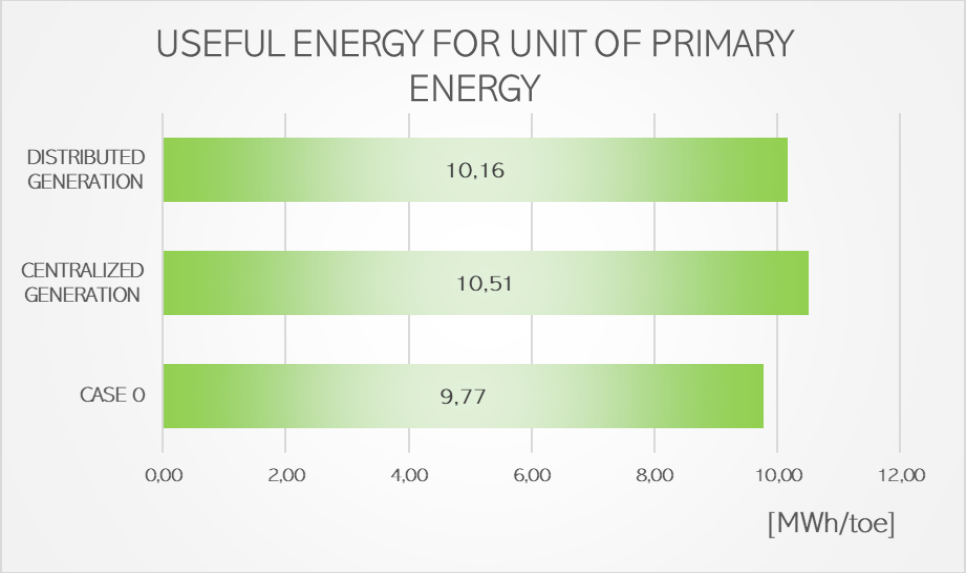

Figure 88: Index of efficiency: how much useful energy is provided to the system [MWh] with one toe of primary energy

It is a sort of efficiency (ϵ), with the primary energy calculated in *toe* with the objective of highlight the primary energy utilization.

$$\epsilon = \frac{E_{useful}\,[MWh]}{E_{primary}\,[toe]} \tag{129}$$

For the evaluation of E_{useful} the control volume ends at the inlet and outlet of secondary supply and return: it is practically the energy provided to the water at the level of substations for district heating and boilers for case 0, and it corresponds to the energy sold.

It is clear how in this case the district heating is better than burning directly natural

gas for heating up water: the energy utilization is higher, and more or less equal for case 1 and case 2, with a slight difference of 3%, due to the higher primary energy consumed in case 2, although the useful energy of case 2 is higher.
It must be remembered that in this work all the energy provided to the district heating network has been produced in the plant. In real cases, in fact, it is possible to exploit the waste heat from industries or other plants, renewable energy sources etc. All these solutions do not have Carbon Dioxide at he output, so they are "free". This mix of solutions in real installations is the reason of the 3-4% of CO_2 emissions saving that was mentioned in the introduction.

6.2 Economic assessment

In this section the results of economic analysis will be discussed.

The first and most immediate parameters are the Net Present Value and the Pay Back Period, calculated in section 5.

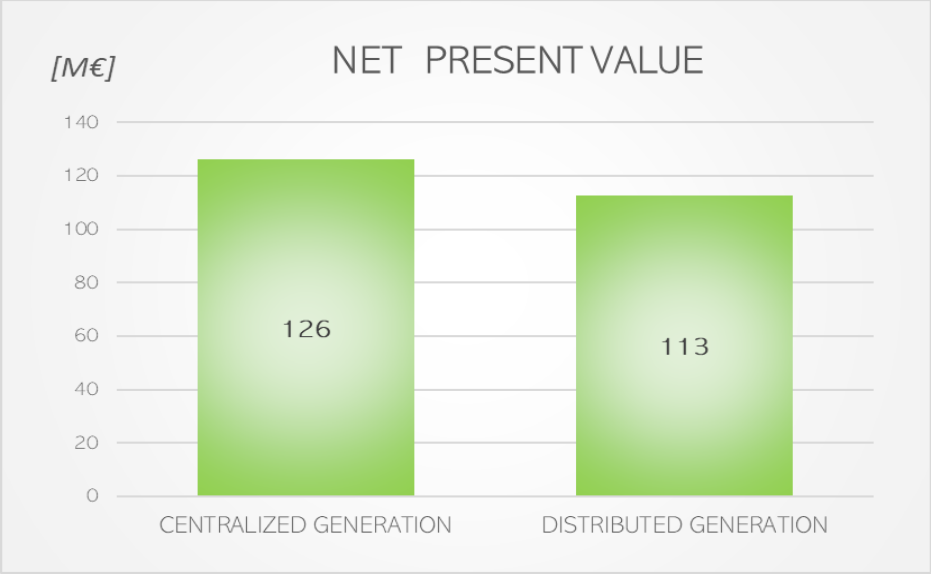

Figure 89: Compared NPV for the two configurations

As it can be noticed for both parameters the better case is the case of centralized generation: the investment returns in less time and with a higher amount of money.

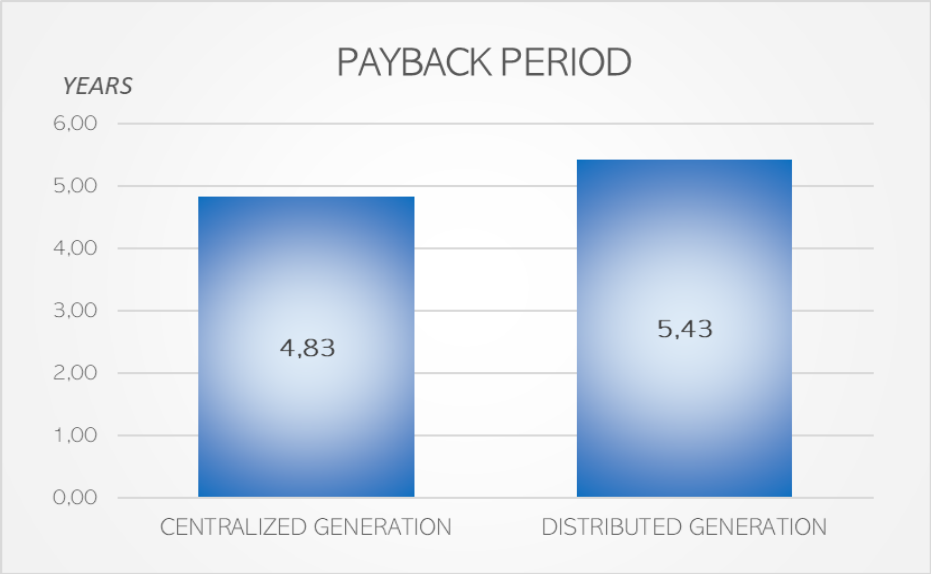

Figure 90: Payback Period of the two configurations

The objective of this section is to find a reason why the centralized generation, in the way it is implemented in this work, presents better results under the point of view of economic investment. As already explained, the distributed generation allows to reduce thermal loss of about 15%, but this is not a variation enough remarkable for the global economic and also technical analysis. The second configuration is composed of 21 thermal boosters, the auxiliary boiler and the main plant, so the thermal power production is divided in 23 total plant, which has obviously a lower power. Leaving unchanged the side investment like pumping system and installation of the network, the scale economy rules impose that many little plants are less economic convenient than a single big plant, and in the following paragraphs this concept will be analyzed more in detail.

	CENTRALIZED GENERATION	*DISTRIBUTED GENERATION*
Initial investment [€]	45,000,000	56,176,092
Unit investment cost [k€/MWe]	1000	1100 - 1650
Annual costs [€/y]	17,167,969	20,135,178
$Incomes_{el}$ [€]	8,262,062	9,911,947

Figure 91: Some details of economic analysis

The values in figure 91 are concerning only the energy production: pumping system and distribution network are excluded. The reason is the willing to focus only on the parameters that cause the differences, and the items excluded are equal in the two cases, so they do not affect the analysis that is going to be performed.

From the figure 91 are taken the reasons of the convenience of invest in the centralized energy production configuration, that are analyzed in detail here:

- INITIAL INVESTMENT

  The first difference between the two cases is already in initial investment. As already said, this is due to the economy of scale rules. The unit investment cost, in fact, is lower in the case of centralized generation. The presence of a big plant reduces the cost per unit of energy, even of 50% for the smaller size plants.

- ANNUAL COSTS

  The situation is the same for O&M annual costs, around 7 €/MWh per year for distributed generation and 36,400 €/MWe per year. This causes a difference in the annual costs of about 3 million euro, tha multiplied by 20 year of lifetime is anything but negligible.

- INCOMES

  While the incomes from the sale of heating is equal in the two cases because connected to the users thermal demand, in case 2 the incomes from the sale of electricity is 1.5 million of euro higher. This is due to the higher percentage of heat provided with cogeneration: in the table of figures 64 and 72 is evident how the percentage of heat provided with the boiler (so without cogeneration) is about 22% in case 2 and about 36% in case 1. This last higher percentage means that a higher amount of heat is provided without correlated production of electrical energy, from this the lower incomes. But the higher incomes do not compensate the higher initial investment.

7 Conclusions and Future Developments

At the end of this work it is clear how the investment in district heating network is convenient under an economic point of view but also for an ecological issue, and all these without a real social consequence: users do not have to change their habit or time.

The most immediate term of comparison is the global efficiency of the system, as it has been calculated in equation (129). In this case the centralized generation is 7.5% higher than case 0 without DHN and 3.5% higher than case 1 with distributed generation, as clarified by figure 88. So the conclusion is that with district heating it is possible a better use of energy and a more efficient heating generation, as it is possible to notice in figure 87, with a reduction of primary energy consumption for generation of heat of about 35-40%.

Another kind of efficiency that can be analyzed is the district heating network intended as thermal losses saving. In this case the comparison is between case 1 and case 2, whose thermal losses are in figure 92.

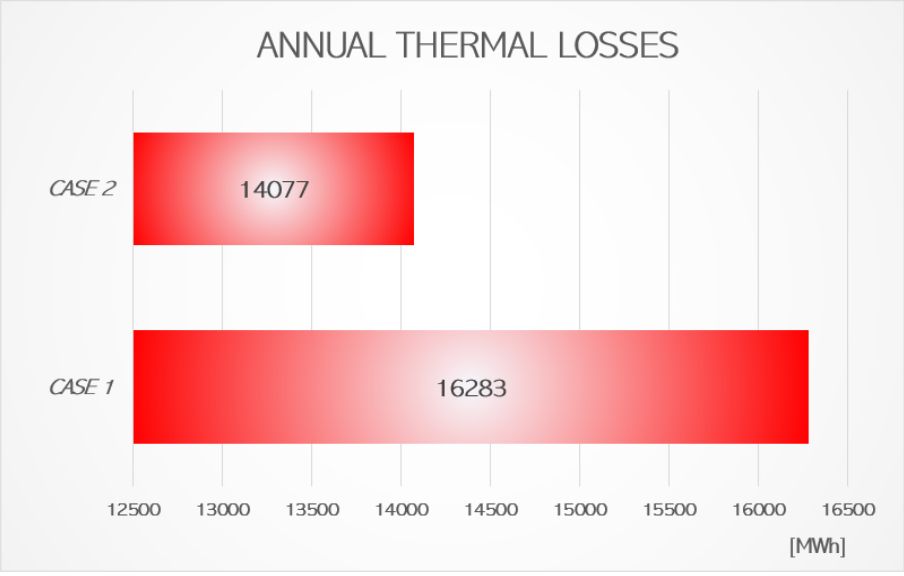

Figure 92: Thermal losses in a year of the two configurations

The reduction of the losses is around 16% between the two cases. Is this saving

enough in order to justify the higher investment and the lower efficiency of smaller size plants?

The answer at this question is no, as both the economic part and the technical part demonstrate:

- The NPV is higher in case 1 of about 10%;
- The CO_2 emissions are higher in case 2 of about 11% while the energy utilization (equation (129)) is lower in case 2 of 3.5% as already said before. This lower percentage of difference is due to the higher electricity production in case 2.

This means that if the energy generation system is supposed to go toward a distributed configuration, the efficiencies of small size plants must be higher. This open the door for the continuation of this study, changing the thermal boosters technology, as explained in next chapter.

7.1 Future developments

At this point, once the conclusions are drawn, it would be interesting to analyse more in detail the different possibilities in order to heat up the water along the line. In fact the critical problem of the distributed generation system is the efficiency of the single plants, that defeats the advantage of having lower thermal losses in the district heating network and more flexibility for the user management. So as future developments, a possible solution to this problem is trying to analyze the different technology available, and studying the behaviour of other energy networks.

The starting point would be the thermal demand, output of the model used in this work (figure 93).

From here, one can choose to heat up the water with a lot of other technologies:

- HEAT PUMP WATER HEATER

  Heat pump water heaters use electricity to move the heat from a lower tem-

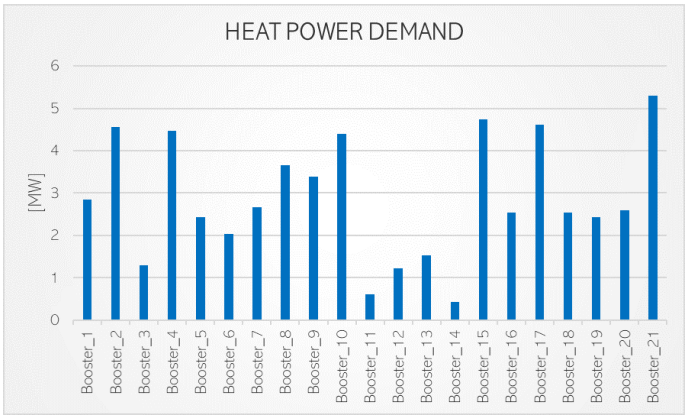

Figure 93: Thermal demand of the boosters

perature level to a higher one. Therefore, they can be two to three times more energy efficient than conventional electric resistance water heaters. To move the heat, heat pumps work like a refrigerator in reverse configuration.
Moreover these systems do not have a direct emission factor, but it depends on the global electric energy generation.

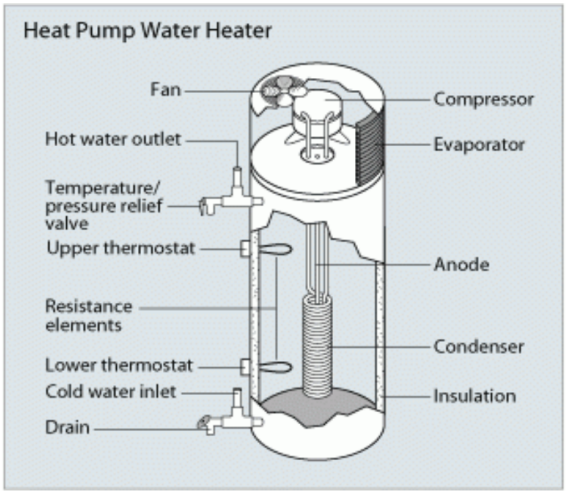

Figure 94: Heat pump water heater scheme [32]

- SOLID OXIDE FUEL CELL

  The fuel cell are an interesting Combined Heat and Power production items. In a contest of zero emissions, the fuel cell can be fed by hydrogen producing

heat and power, with zero CO_2 emissions.

Alternatively, for a connection with gas network, it can be fed by methane and hydrogen but in this case there is a Carbon Dioxide emission.

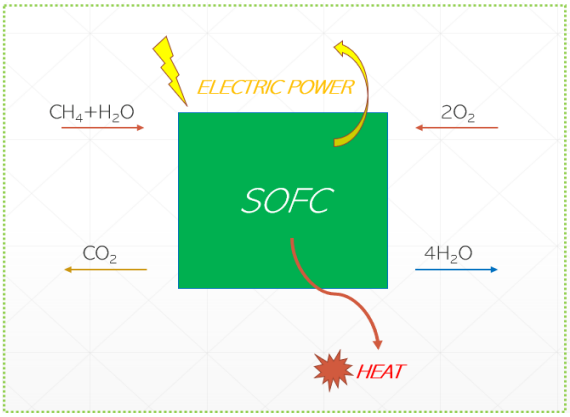

Figure 95: Solid Oxide Fuel Cell basic operation scheme

As already said, an integrate analysis of energy network would be very interesting. In order to do that it is sufficient to extract the values of gas and electricity consumption for each user node, and using them as input for the network simulation. The point is that every technology would have its own primary energy consumption and its own output, in addition a comparative economic analysis would highlight the different state of art of each different technology in the actual period.

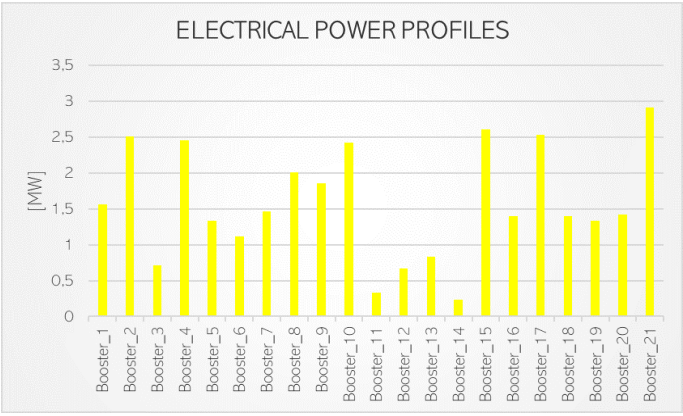

Figure 96: Electricity output of each booster

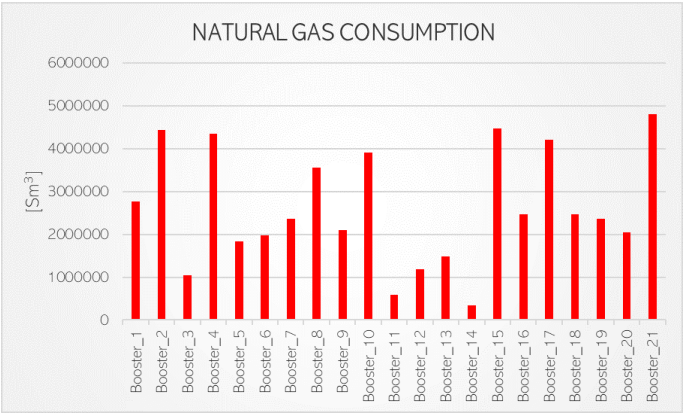

Figure 97: Natural gas consumption of each booster

For the CHP plants described in this work, the analysis would start from this inputs.

References

[1] https://www.gruppohera.it/gruppo/com_media/dossie_tlr/articoli/pagina 70.html

[2] *DHC + Technology Platform, District heating and cooling. A vision toward 2020-2030-2050*, March 2012.

[3] *Future district heating systems and technologies: On the role of smart energy systems and 4th generation district heating*, Lund et al.

[4] *Dynamic modelling of local district heating grids with prosumers: A case study for Norway*, Kauko et al.

[5] *Energy storage and smart energy systems*, Lund H, Østergaard PA, Connolly D, Ridjan I, Mathiesen BV, Hvelplund F, et al.

[6] *Computational comparison of a novel decentralized photovoltaic district heating system against three optimized solar district systems*, Hassam ur Rehman, Janne Hirvonen, Risto Kosonen, Kai Sirén

[7] *CHP and heat pumps to balance renewable power production: Lessons from the district heating network in Stockholm*, Fabian Levihn

[8] *District heating based on biogas from wastewater treatment plant*, Alberto Picardo, Victor M. Soltero, M. Estela Peralta, Ricardo Chacartegui

[9] *Numerical Design of Thermal Systems*, A.Sciacovelli, V. Verda, R.Borchiellini

[10] Del Hoyo Arce I., Herrero Lopez S., Lopez Perez S., Rama M., Klobut K., Febres J. A., *Models for fast modelling of district heating and cooling networks*, Renewable and Sustainable Energy Reviews 82 (2018) 1863-1873.

[11] *Le equazioni della meccanica dei fluidi*, Stefano Lanzoni

[12] *Thermo-fluid dynamic model of large district heating networks for analysis of primary energy savings*, Guelpa E., Sciacovelli A., Verda V., Energy (2017)

[13] *Numerical model for the analysis of thermal transients in district heating networks*, Capone, Guelpa, Verda

[14] *Dynamic modeling and control of a plate heat exchanger*, Hector Bastida, Carlos Ernesto Ugalde-Loo, Muditha Abeysekera, Meysam Qadrdan

[15] *Studio di una Rete di Teleriscaldamento nel Comune di Padova*, Lorenzo Casna

[16] https://www.airu.it/teleriscaldamento/

[17] *Valutazione del potenziale nazionale di applicazione della cogenerazione ad alto rendimento e del teleriscaldamento efficiente*, GSE

[18] *Cost Estimation Methodology for NETL Assessments of Power Plant Perfomance*, NETL

[19] *Energia elettrica, anatomia dei costi*, RSE Riflessioni sull'Energia

[20] *Combined Heat and Power*, IEA-ETSAP

[21] https://www.pumpsandsystems.com/estimate-pump-installation-costs

[22] https://www.arera.it/it/dati/gpcfr2.htm

[23] *Dispensa del corso di "SISTEMI ENERGETICI". Argomento: Sistemi Energetici (parte 3.2)*, Prof. Pier Ruggero Spina, Dipartimento di Ingegneria Università di Ferrara

[24] https://mercati.ilsole24ore.com/tassi-e-valute/valute/contro-euro/cambio/EURUS.FX

[25] MATTM, https://www.minambiente.it/

[26] http://www.isprambiente.gov.it/

[27] *TESTO INTEGRATO DELLE DISPOSIZIONI PER LA REGOLAZIONE DELLE PARTITE FISICHE ED ECONOMICHE DEL SERVIZIO DI BILANCIAMENTO DEL GAS NATURALE (TISG)*, ARERA (Autorità di Regolazione per Energia Reti e Ambiente)

[28] *Piano per il riscaldamento ambientale e il condizionamento della Regione Piemonte [Aggiornamento del Piano regionale per il risanamento e la tutela della qualità dell'aria: Stralcio per il riscaldamento ambientale e il condizionamento e disposizioni attuative della legge regionale 28 Maggio 2017 n. 13 (Disposizioni in materia di rendimento energetico nell'edilizia)* - Articolo 21, lettere a), b) e q)]

[29] *Sistemi di teleriscaldamento*, Vittorio Verda, Dipartimento Energia - Politecnico di Torino, lecture slides of the course "Complementi di Energetica"

[30] *Studio e caratterizzazione di un modello compatto per l'analisi di sottostazioni di scambio termico di teleriscaldamento*, Daniele Farina. Relatore: Prof. Vittorio Verda, Correlatore: Ing. Elisa Guelpa

[31] Università degli Studi di Napoli Federico II, D.E.TE.C. - Dipartimento di Energetica, *Cogenerazione e trigenerazione: dai principi generali alle applicazioni*, Gestione delle Risorse Energetiche, A.A. 2012/2013

[32] https://www.energy.gov/energysaver/water-heating/heat-pump-water-heaters